Journal of Energy Storage 132 (2025) 117705

Contents lists available at ScienceDirect

Journal of Energy Storage

journal homepage: www.elsevier.com/locate/est

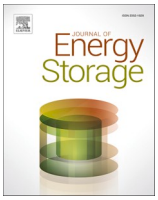

Research Papers

Life cycle assessment of a novel hybrid energy storage system: Environmental hotspots and sustainability options based on experimental insights

Eva-Maria Heigl [a,*], Michael Schäffer [b,c], Lukas Zeilerbauer [a,d,e], Andreas Zauner [a], Johannes Lindorfer [a], Johannes Ott [b,c], Peter Fischer [b,c]

[a] Energieinstitut an der Johannes Kepler Universität Linz, Altenberger Straße 69, 4040 Linz, Austria
[b] Department of Applied Electrochemistry, Fraunhofer Institute for Chemical Technology, Joseph-von-Fraunhofer-Straße 7, 76327 Pfinztal, Germany
[c] German-Australian Alliance for Electrochemical Technologies for Storage of Renewable Energy – CENELEST, University of New South Wales, Sydney, Australia
[d] Institute for Chemical Technology of Organic Materials (CTO), Johannes Kepler University Linz, Altenberger Straße 69, 4040 Linz, Austria
[e] Institute of Polymeric Materials and Testing (IPMT), Johannes Kepler University Linz, Altenberger Straße 69, 4040 Linz, Austria

ARTICLE INFO

Keywords:
Hybrid energy storage system
Stationary electric energy storage
Sustainable materials
Vanadium redox flow battery
Supercapacitor
Life cycle assessment
Circular economy
Grid flexibility
Energy transition

ABSTRACT

This article reports on the life cycle assessment (LCA) of a novel hybrid energy storage system (HESS) for stationary use. The system combines a vanadium redox flow battery (VRFB) with a supercapacitor, simultaneously delivering high energy and high power. The LCA aimed to identify environmental hotspots in the HESS lifecycle and to provide recommendations for an environmentally-sustainable technology deployment. New life cycle inventory (LCI) datasets for the supercapacitor and DC-DC converters were created based on manufacturer data. A focus was laid on vanadium pentoxide (V_2O_5), the active component in the VRFB's electrolyte with significant environmental impacts. Existing LCI datasets for primary and secondary V_2O_5 production were evaluated regarding their quality and applicability. Additionally, a new laboratory scale process for recycling of waste vanadium electrolyte was developed and served as input for the LCA. The recycled electrolyte, which can be directly used in VRFBs, had a global warming potential (GWP) of 0.91 kg CO_2-eq/kg at a vanadium concentration of 1.6 mol/l. The LCA of the HESS lifecycle for a real use case showed a GWP ranging from 0.10 to 0.53 kg CO_2-eq/kWh, depending on scenario. V_2O_5 and the electricity losses during dis−/charging were identified as main environmental hotspots. The overall impacts of the system could be significantly reduced, if using recycled instead of primary vanadium electrolyte and renewable instead of conventional electricity sources for charging. The findings of this study underscore the importance of sustainable V_2O_5 sourcing and a circular economy for vanadium electrolyte to support the environmentally-sustainable market deployment of the HESS.

1. Introduction

The European Green Deal targets the decarbonization of the European energy system and aims at "developing a power sector based largely on renewable sources" [1]. The evolving energy transition poses many new challenges for grids, owing to the volatile nature of renewables. One of them is the increasing need for stationary power storage [2]. This calls for innovative approaches, which have to be sustainable themselves. The European Battery Regulation (Regulation EU 2023/1542) [3] adopted in 2023, promotes circular economy in battery value chains, thus supporting the Sustainable Development Goals of the UN (SDGs) [4] and the Paris Agreement targets on climate change [5]. The regulation aims at making "batteries sustainable throughout their entire life cycle – from the souring of materials, to their collection, recycling and repurposing" [3]. Starting from 2025, it will be mandatory to create a carbon footprint declaration for various types of batteries. For industrial rechargeable batteries with external storage, such as vanadium redox flow batteries (VRFBs), this obligation will enter into force by 2030. The European Battery Regulation contains a variety of additional obligations, for example regarding the recycled content of batteries or minimum recycling rates for certain materials contained in batteries, such as nickel [3,6]. Supercapacitors (SC), based on a different energy storage mechanism than batteries, are not subject to the Battery Regulation; however, similar obligations might apply to them in the future. Hence, it is indispensable to include sustainability considerations

* Corresponding author.
E-mail address: heigl@energieinstitut-linz.at (E.-M. Heigl).

https://doi.org/10.1016/j.est.2025.117705
Received 30 September 2024; Received in revised form 21 June 2025; Accepted 9 July 2025
Available online 22 July 2025

Nomenclature

AC	alternating current
BC	battery converter
BMS	battery management system
CAS	Chemical Abstracts Service (by the American Chemical Society)
CC	current collector
CMR	cancerogenic, mutagenic and reprotoxic
CRM	critical raw material
DC	direct current
DEHPA	di(2-ethylhexyl)phosphoric acid, IUPAC name: bis(2-ethylhexyl) hydrogen phosphate
EES	electrical energy storage
EMS	energy management system
EST/S	energy storage technology/system
EOFP	photochemical oxidant formation potential - ecosystems
EoL	end-of-life
ES	end-of-life scenario
EU	European Union
FB	flow battery
FEP	freshwater eutrophication potential
FETP	freshwater ecotoxicity potential
FFP	fossil fuel potential
g	gross
GHS	Globally Harmonized System of Classification, Labelling and Packaging of Chemicals (UN)
GWP	global warming potential
HESS	hybrid energy storage system
HOPF	photochemical oxidant formation potential - human health
HP	high power
HTPc	human toxicity potential - cancer
HTPnc	human toxicity potential - non-cancer
IRP	ionizing radiation potential
LCA	life cycle assessment
LCA for Experts	a software for LCA modeling
LCI	life cycle inventory
LCIA	life cycle impact assessment
LED	light emitting diode
LIB	lithium-ion battery
LOP	agricultural land occupation potential
LTO	lithium titanite oxide
METP	marine ecotoxicity potential
n	net
NCA-C	lithium nickel cobalt aluminum oxide cathode and graphite anode
NCO-LTO	lithium nickel cobalt oxide cathode and lithium titanite oxide anode
NMC	(lithium) nickel manganese cobalt oxide
nr	non renewable
ODP	ozone depletion potential
PCS	process control system
PED	primary energy demand
PMFP	particulate matter formation potential
PS	production scenario
PV	photovoltaic/s
r	renewable
rec.	recycled
ReCiPe 2016	a harmonized LCIA methodology
SC	supercapacitor
SCC	supercapacitor converter
SDGs	Sustainable Development Goals of the UN
SMS	supercapacitor management system
SOP	surplus ore potential
TAP	terrestrial acidification potential
TETP	terrestrial ecotoxicity potential
TRL	technology readiness level
V_2O_5	vanadium pentoxide
VRFB	vanadium redox flow battery
w/c	with credit(s)
WCP	water consumption potential

already in the development phase of new batteries or other energy storage systems.

VRFBs are an excellent option for large-scale stationary electrical energy storage, with easy and independent scalability of power and energy. Moreover, they exhibit good safety properties because of the use of a non-flammable, water-based electrolyte that employs only one metallic element in its active compound, namely vanadium [7–9]. VRFBs allow for easier dismantling and recycling and usually have a longer lifetime than lithium-ion batteries (LIBs) [9]. LIBs currently present the most applied energy storage technology (EST) for battery electric vehicles and consumer electronics, with superior performance characteristics, such as high power and energy density [10]. However, owing to persistent safety concerns, raw material scarcity and other issues, it is unclear, whether this battery type will be widely implemented in grid-scale stationary applications in the future [10,11]. The dis−/charging times of VRFB are on the scale of up to a few hours [12]. SC, on the other hand, feature a lower energy density than VRFB, while providing a higher power density with faster dis−/charging and a superior storage efficiency [12,13]. The fundamental working principles of VRFB and SC are described elsewhere in literature [13–17].

The project presented here combines the advantages of a VRFB and a SC by hybridizing these two energy storage technologies (ESTs). This simultaneously allows for the fast handling of high loads through the SC and provides a high storage capacity through the VRFB. This novel hybrid energy storage system (HESS) can for example support grid flexibility, by balancing the electricity supply from renewable sources. The HESS was demonstrated on laboratory and industrial scale in the project HyFlow [18], which was conducted by an international project consortium from 2020 to 2024 and funded by the European Union's Horizon 2020 research and innovation program. The system's functionality and component compatibility was validated by testing the developed energy management algorithm and control strategies and simulating different load profiles. As part of this project, a life cycle assessment (LCA) was conducted on the HESS industrial demonstrator, with the aim to identify environmental hotspots in the system's entire lifecycle and to provide recommendations for an environmentally-sustainable technology deployment.

The LCA of the HESS proved to be complex, owing to several main components and a high number of sub-components that needed to be assessed. While for VRFBs many LCA studies – some of them providing very transparent data – have already been published, i.a. [7,19–24], there is only little LCA data available on SC [23,25–27], DC-DC converters, AC-DC inverters or hybrid energy storage systems. Dieterle et al. [8] provided a comprehensive overview of publications on LCA of flow batteries (FB) and discussed methodological decisions. Their recommendations on the LCA study design for FBs were considered for our study. Ebner et al. [11] asked the question “How green are redox flow batteries?” and created a valuable overview of available LCA studies. Jiao et al. [26] performed an LCA of the application of different hybrid energy storage systems to a future 100 % renewable power system.

Using primary data directly provided by manufacturers, we developed new LCI datasets for the SC and the DC-DC converters, thus

addressing gaps in the existing literature.

Regarding the VRFB, other publications already demonstrated that the electrolyte, specifically due to its active component vanadium pentoxide (V_2O_5), has a high impact on the lifecycle LCIA results of the VRFB [7,20–22]. Moreover, vanadium has been on the list of critical raw materials (CRM) of the EU [28,29] since 2017 [30]. CRMs are considered as essential for European economy, while their supply may be at risk for geopolitical, geological or geographical reasons. In 2020, approximately 72 % of global vanadium production occurred as co-production with steel-making, 18 % was direct vanadium mining and 10 % originated from secondary sources [31]. Vanadium mining, direct or as co-product, takes place in a few countries only, all of which are outside of Europe, mainly China, South Africa and Russia [8,16,32]. The current geopolitical situation adds even more stress on the supply situation. One strategy to cope with supply and scarcity risks and to reduce environmental impacts is the further development of a circular economy. Secondary sources of vanadium are spent chemical process catalysts, residues of burnt crude oil or vanadium-containing steel scrap, with the latter being the largest vanadium sink and possibly also representing an important source of recycled vanadium in the future. Currently, vanadium is mainly recycled via the steel route in a steel alloy form, not as a high-purity metal, getting lost over time due to “dilution” for lack of separate collection of vanadium-containing steel scrap [33]. Apart from the already mentioned secondary sources, energy storage applications, such as VRFBs, are gaining more importance and thus will likely also present relevant sources - and sinks - of recycled vanadium in the future [33].

Hence, we set a focus on this critical component in our study, analyzing its possible impact on the HESS in more depth. We identified several datasets for primary and secondary V_2O_5 production in the existing literature, evaluating their quality and applicability for our study.

Vanadium electrolyte recycling seems a logical approach, with the waste raw material being available in an easily accessible form. A recent book on emerging battery technologies by Passerini et al. [2] identified worldwide installed VRFB systems of 1.23 GWh and 319 MW in 2020. Until 2022, the installed capacity rose to approximately 1.8 GWh and is expected to further increase to 33 GWh by 2031 [34]. The defossilization of our energy system will trigger a growing demand for stationary energy storage [2,35]. Consequently, it is assumed that the market share of VRFBs will increase from 1.8 % in 2020 to 5 % by 2050. While at the moment the supply of spent electrolyte might be miniscule compared to its demand, it is expected to grow in the upcoming years along with the installed VRFB storage capacity; albeit with some delay due to the long lifetime of the VRFB and its electrolyte. Moreover, the approach of electrolyte recycling fits well into the electrolyte leasing business model that suppliers are starting to pursue [36].

Several publications have already discussed the topic of vanadium electrolyte recycling or tried to approximate its potential environmental benefits [20–22,33], however, so far only one has performed an LCA of the recycling process: Blume et al. [37] recently reported on the LCA of recycling of spent vanadium electrolyte in four different EoL states, observing reduction potentials of up to 100 % in GWP compared to primary electrolyte.

To contribute to this relevant field of research, we developed and demonstrated a laboratory scale process for waste electrolyte recycling, thus deriving novel inventory data for our LCA.

Eventually, we assessed the environmental impacts of the entire HESS lifecycle for a real use case in German industry in several scenarios: We applying selected V_2O_5 LCI datasets from literature and the recycled vanadium electrolyte of this study to our HESS LCA model and used different electricity sources, conventional and renewable, for charging of the HESS. By identifying the most important environmental hotspots in the lifecycle of the system, we were able to derive important preconditions for an environmentally-sustainable market deployment of this novel EST.

To the best of our knowledge, the present article is the first to report on an LCA of a stationary HESS in a VRFB-SC configuration that has actually been demonstrated on an industrial scale. Other distinguishing features of this LCA are the focus on the critical raw material V_2O_5, supported by laboratory tests on waste vanadium electrolyte recycling, and the primary data provided by manufacturers.

2. Materials and methods

In this study, an LCA of a novel energy storage system was performed, with input data partly generated through laboratory tests.

2.1. Life cycle assessment

The production, use and end-of-life phases (EoL) of a novel HESS, integrating a VRFB with a SC, were analyzed through LCA. A special focus was placed on the environmental impacts of the critical component V_2O_5. LCA was carried out following the ISO 14040/14044 methodology [38,39], which encompassed the subsequent working steps: definition of goal, scope and system boundaries of the LCA, compilation of the LCI, life cycle impact assessment (LCIA) and interpretation and discussion. Additional details on the applied methodology are provided in standard works such as Frischknecht et al. [40], Guinée et al. [41], Curran (Ed.) [42] or Klöpfer and Grahl [43].

2.1.1. Definition of goal and scope

This LCA aimed to identify environmental hotspots in all lifecycle phases of the HESS industrial scale demonstrator, and to derive recommendations for an environmentally-sustainable roll-out of this novel technology. Important inventory data for the LCA were provided by component manufacturers, and compiled from literature, with a focus on the critical raw material V_2O_5. Input data for the LCA were partly derived from laboratory tests on the recycling of waste vanadium electrolyte, as described in chapter 2.2. The content and structure of this study is outlined in Fig. 1.

This article mainly focuses on the environmental impact category “climate change” with its indicator GWP and on the primary energy demand (PED). However, we determined indicator values for a number of other categories, which were made available in the Supplementary Information (SI). The industrial scale HESS demonstrator that was subject to this LCA is schematized in Fig. 2.

The LCA of the HESS encompassed its production, use and EoL phases. This included raw material supply (mining/extraction from nature), energy supply (natural gas extraction, electricity generation etc.), manufacturing of precursor materials, manufacturing of HESS components, assembly of the HESS, the use phase of the HESS, and its disposal or recycling, including all transport steps. Infrastructure was considered in the assessment, if appropriate information or suitable datasets were available. The manufacturing, use and EoL of the HESS were assumed to take place in Europe; therefore, the geographical system boundary was Europe. In case of raw materials that are sourced from other regions of the world, transportation to Europe was accounted for. The functional unit (FU) of this LCA was defined as 1 kWh of total energy delivered by the HESS over its lifetime. This is consistent with the FU definition for the carbon footprint declaration of batteries under the European Battery Regulation [3]. The LCA was performed for a real use case of peak shaving in German industry over 20 years.

2.1.2. Life cycle inventory data

This chapter contains information on the compilation of LCI data for all lifecycle phases of the HESS. LCI data – specifically for the production phase – were to a large extent provided by project partners from either laboratory tests, newly developed components or commercial products. Gaps were filled with valid literature data. Datasets on background processes were derived from the Sphera Professional Database 10.7 [45] and ecoinvent v3.8 database [46]. LCI datasets from Europe were

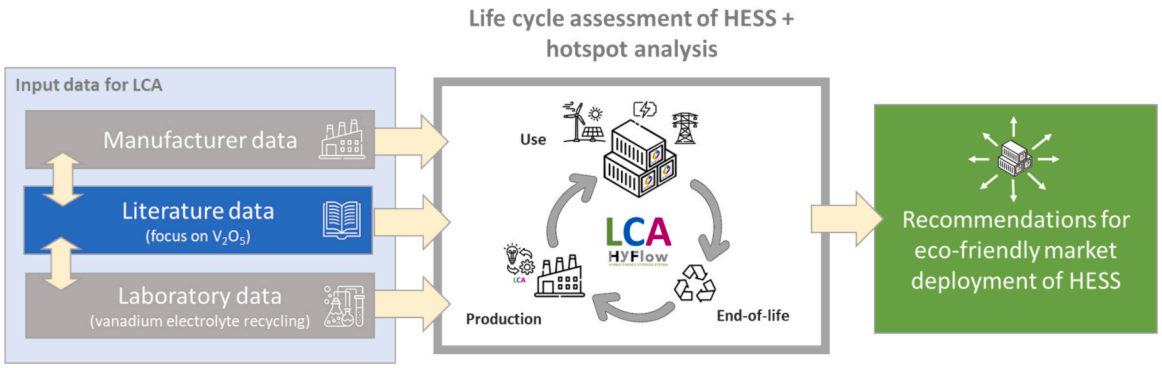

Fig. 1. Content and structure of this study (icons provided by [44]).

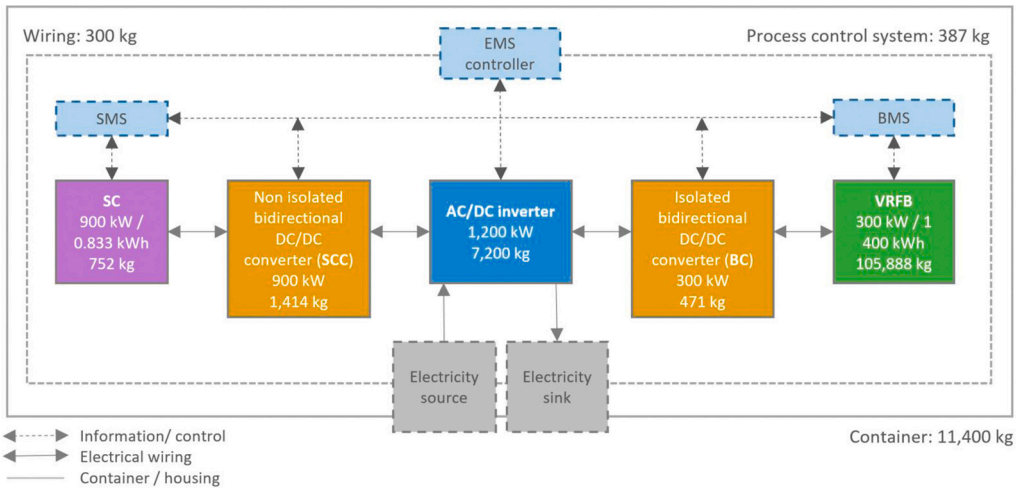

Fig. 2. Schematic representation of the industrial scale HESS demonstrator.

preferred for this LCA, if available. Special emphasis at this stage was placed on the evaluation of existing LCI datasets for the critical component V_2O_5. The foreground LCI for the industrial scale HESS, as visualized in Fig. 2, as well as all other inventory tables are provided in the SI.

2.1.2.1. Production of VRFB. A commercial VRFB was installed for the industrial scale HESS demonstrator in this project. However, the LCA was performed for the upscaled laboratory setup to incorporate the achieved technological advances at the laboratory scale, such as thinner VRFB membranes. Some components, including electrolyte tanks, pumps, pipes or cables, were approximated based on product datasheets. The vanadium electrolyte had an energy density of 20 Wh/l, a density of 1.35 kg/l and a vanadium concentration of 1.6 mol/l. The LCI of the industrial scale VRFB, the methodology for upscaling the LCI from laboratory to industrial scale, as well as the inventories of all used background processes, are provided in the SI.

2.1.2.2. Production of the active electrolyte component V_2O_5. Table 1 lists V_2O_5 datasets available in the existing literature, indicating their most important parameters. Only references with proprietary V_2O_5 datasets are mentioned. We want to specifically point out the publication by He et al. [7], who compared V_2O_5 datasets from three different articles [21,47,48].

Weber et al. [21] described a process in South Africa, starting from the extraction of titanomagnetite ore and yielding "high purity" V_2O_5 as a by-product of electric arc furnace steel production, without detailing the achieved vanadium concentration. They applied economic allocation in a significant process step, which turned out to be problematic because of large variations in results possible with volatile market prices. This has already been noted by Blume et al. [20]. Blume et al. [20] based their assessment on the same mine in South Africa; however, they solved the multi-product system of the steel-vanadium production process through system expansion by assigning credits for primary steel, delivering high purity V_2O_5 (97.5 %). He et al. [7] applied the following V_2O_5 datasets to model their VRFB: Primary V_2O_5 as a by-product of hard-coal consuming blast furnace crude steel making from titanomagnetite ore, based on data from Chen et al. [47] of a real plant in China (time horizon 2005–2007) (scenario A1). This dataset does not consider the allocated impact of steel-making. Moreover, the degree of purity of the obtained V_2O_5 is not mentioned, leaving it open whether further concentration steps would be necessary for application in VRFB electrolytes. They also applied data from Jungbluth and Eggenberger [48] on V_2O_5 production from residues of a power plant burning crude oil based on real data (scenario A3) and stoichiometric calculations (scenario A4). The impact of crude oil production and burning was not considered. For their scenario analysis, Li et al. [49] performed an LCA of the production of high-purity (>98 %) V_2O_5 nanosheets for electrochemical applications from conventional and secondary sources; the first was based on stoichiometric calculations for vanadium extraction from vanadium containing ore in China, excluding the impact of ore mining. The second referred to a laboratory scale vanadium recovery process from gasification waste (carbon soot) of a Singaporean oil refinery. The carbon soot was modeled free of environmental burden. Zhang et al. [32] described a sodium roasting, calcium roasting and submolten salt production process, all taking place in China and starting

Table 1
Existing LCI datasets for V_2O_5 production from primary and secondary sources, ctg = cradle-to-gate, gtg = gate-to-gate.

GWP [kg CO_2-eq/kg]	Reference	V_2O_5 source		Location	LCA scope	V_2O_5 purity [%]	LCIA results provided	LCI provided	LCIA methodology
11	Chen et al. [47] (as applied by He et al. [7])	Prim	Titano magnetite (blast furnace steel making, prod. data from 2005 to 2007, allocated impact of steel making not incl.)	China	gtg	Not indicated	Yes	Yes	CML2001
2 (real plant data) 1 (stoich. calc.)	Jungbluth and Eggenberger [48] (in He et al. [7])	Sec	Oil burner residues	Japan	gtg	Original full-text publication by Jungbluth and Eggenberger [48] could not be found; LCIA results but no LCI were provided by He et al. [7]			
19 (original) 7 (new economic allocation factors)	Weber et al. [21]	Prim	Titano magnetite ore (electric arc furnace steel making)	South Africa	ctg	"High" purity	Yes	Yes	CML2001
28	Li et al. [49]	Sec	Gasification waste from oil refinery (carbon soot)	Singapore / China	gtg	>98	Endpoint only	Yes	ReCiPe 2016 endpoint
66	Li et al. [49]	Prim	Vanadium containing ore (stoich. calc.), excl. mining	China	gtg	>98	Endpoint only	Yes	ReCiPe 2016 endpoint
95	Blume et al. [20]	Prim	Titano magnetite ore (electric arc furnace steel making)	South Africa	ctg	97.5	Yes	Yes	CML2001
63: P I 18: P II 48: P III	Zhang et al. [32]	Prim	Titano magnetite ore (LCA starting from V slag)	China	gtg	"High" purity	Yes	Yes	Midpoint results, method not indicated
115	Shakibania et al. [50]	Sec	Spent oil-refinery catalysts (lab tests)	Iran	gtg	>99.5	Yes	No comprehensive table	Presumably midpoint results, method not indicated
27	Baritto et al. [51]	Sec	Bitumen-derived petcoke fly ash (from oil sands)	Canada	ctg	97–98.5	Yes	Yes	Only GWP, IPCC
10	Baritto et al. [51]	Sec	Spent catalysts from bitumen upgrading	No LCI available, only GHG value listed as benchmark, cradle-to-gate					
–	Sphera [45]	Prim	Titano magnetite ore (magnetic separation of ore, sodium metavanadate route)	South Africa	ctg	86	Yes	No (dataset not expandable)	–
–	Sphera [45]	Prim	Titano magnetite ore (magnetic separation of ore, sodium metavanadate route)	South Africa	ctg	98	Yes	No (dataset not expandable)	–

from vanadium slag, hence not a cradle-to-gate scope. Shakibania et al. [50] assessed the production of V_2O_5 (>99.5 %) from Iranian oil-refinery catalysts, stating that their relatively high results i.a. regarding GWP are due to the low technology readiness level (TRL) of their process. Baritto et al. [51] assessed the cradle-to-gate GHG emissions of a recovery process of V_2O_5 at 97–98.5 % purity from bitumen-derived petcoke fly ash in Canada and cited an earlier, apparently unpublished study on the recovery of V_2O_5 from spent catalysts from bitumen upgrading. In addition to the previously mentioned publications on V_2O_5, there also are two primary V_2O_5 datasets of different degrees of purity available in a commercial LCA database [45]. However, they cannot be used for detailed analyses in this study because of license restrictions and only are valid for one major vanadium exporting country.

The identified V_2O_5 datasets show a very wide range of GWP results, even when comparing only primary datasets. This is due to different raw materials, assessed production processes, TRL, degrees of V_2O_5 purity, geographic location of mining and production, applied LCA scope and parameters and data quality. Primary V_2O_5 produced from titanomagnetite ore in South Africa, as described by Blume et al. [20], showed the highest GWP of all primary datasets. Unfortunately, most other primary datasets only describe gate-to-gate processes; hence, they do not cover the entire production chain. For secondary sources, we consider it legitimate to assume the waste raw materials as free of environmental burden. V_2O_5 from secondary sources does not necessarily feature a lower GWP than V_2O_5 from primary sources, especially because of the low TRL of secondary processes. Secondary V_2O_5 from spent oil-refinery catalysts even has the highest GWP of all V_2O_5 datasets. However, most secondary sources show a significantly lower GWP than primary V_2O_5 from South Africa [21], which we consider the most complete and accurate dataset for the production of primary V_2O_5. For all further analyses in this LCA study, we used the two primary cradle-to-gate V_2O_5 datasets, as we wanted to cover the entire production chain, and the secondary dataset for V_2O_5 from Chinese oil refinery carbon soot [49].

2.1.2.3. Production of SC, converters and periphery. A market-ready 25 kW SC developed by a project partner was used as the basis for generating the LCI of the required 900 kW SC. For a SC of 900 kW / 3 MWs and a usable voltage range of 300–900 V, 830 of these SC cells would be required. The SC applies coconut-shell activated carbon-nickel and nickel-steel electrodes and uses a water-based alkaline electrolyte. For confidentiality reasons, the exact composition of this SC cannot be fully displayed in this article.

There are several publications available on the LCA of graphene or activated carbon (AC) for SC electrodes from conventional and renewable sources, that is, [25,52–57]. In our project, a process for the production of AC for SC application from the solid digestate of an Italian biogas plant through pyrolysis-activation was developed and published in a previous article [58]. This approach avoids the import of AC from outside of Europe, such as coconut-fiber-based AC from Asia [52]. While organic electrolytes can increase the achievable voltage window of a SC [59], they may also possess hazardous properties, such as high flammability or health hazards. This is the case for acetonitrile [60] used in three of the four identified SC LCA studies [23,25,26]. Hence in our project, water-based SC electrolytes and water-in-salt SC electrolytes were investigated. Nickel is an essential raw material for EST [61], but causes high environmental impacts in its production phase [62]. It is

also contained in the electrodes of the here investigated SC. Not yet on the CRM list of 2020 due to its well diversified supply situation [63], Nickel was added as a Strategic Raw Material to the EU's fifth CRM list in 2023 [29,64], even if not meeting the CRM threshold [28]. Therefore, we aimed to assess how the use of recycled nickel could improve the environmental performance of our SC. However, it must be emphasized that the developed inventory for nickel recycling, as presented in the SI, represents a rough approximation, based on a very general literature source [62], owing to the lack of other data. When combing through literature, it became apparent that sufficient sourcing of pure recycled nickel might be difficult at present: Nickel is mainly recycled within the steel route, "remaining in a steel alloy form" [65] and "relatively little class I nickel scrap is available for recycling" [66]. Another study states that "nickel stocks in use are growing rapidly, but the long lifetimes of nickel products mean that these stocks will only be available for recycling in a few decades, limiting the chance to replace more primary sources by postconsumer scrap in the near future" [67]. However, the new European Battery Regulation [3,6] will demand the use of a certain percentage of recycled nickel in battery systems applying nickel as active material in the future and will also enforce recycling of nickel components at the EoL of a battery. Hence, the demand for and the availability of recycled battery-grade nickel is expected to increase.

To describe the AC-DC inverter, the ecoinvent 3.8 dataset "inverter production, 500 kW, RER" was applied and linearly upscaled to an inversion power of 1200 kW. The two DC-DC converters were modeled based on a 6.2 kW non-isolated DC-DC converter developed by a project partner, which was also linearly upscaled.

2.1.2.4. Use phase of HESS. The use phase of the HESS was calculated for an application of peak shaving of medium and short duration power peaks in industry, based on a real consumption profile from Germany. In case of high demand peaks from the consumer, the SC is able to (partly) provide these, thus flattening the consumption profile and avoiding grid disturbances through feedback effects. The timeframe of the use phase was 20 years. The electricity supply for charging the HESS was modeled in three scenarios with a conventional European electricity grid mix, wind power and photovoltaic (PV) power.

Moreover, it was assumed that the finished HESS would be transported by truck over an average distance of 600 km to customers within Europe. The replacement of some HESS components within the operational time of the HESS was also accounted for.

The overall storage or energy efficiency of the HESS depends on the specific use case respectively on the degrees of usage of VRFB and SC, and on the individual energy efficiencies of the single components (Table 2). The VRFB has the largest impact on the overall system efficiency, as it is the component with the lowest individual energy efficiency and buffers most of the energy drawn from the grid during operation. To determine the theoretical limits of the HESS energy efficiency, we assessed the four possible storage pathways, assuming that the entire energy charged from the grid passes all indicated components. The storage pathways are described in Table 2 and a visualization is provided in the SI. The resulting theoretical energy efficiency of the HESS ranges from 43 % to 79 % (Table 2). However, pathways 3 and 4, showing the extreme efficiency limits, do not represent reasonable continuous applications of the HESS and only occur during very short periods of time. For our use case, a mean energy efficiency of 60 % over 20 years was approximated, as the largest share of the charged energy passes the VRFB and only a minor share additionally passes the SC *or* is only charged and discharged via the SC. Uncertainties with respect to the system's energy efficiency were addressed in a sensitivity analysis (chapter 2.1.4).

Table 2
Mean values for energy efficiency of HESS components and limits of overall energy efficiency of HESS.

Component	Energy efficiency	Description of storage pathway
HP-VRFB	75 %[1]	–
SC	>95 %[2]	–
AC-DC inverter	97 %[3]	–
BC	93 %[1]	–
SCC	94 %[1]	–
Overall HESS energy efficiency		
Pathway 1	61 %	Slow charging and discharging via VRFB, no use of SC
Pathway 2	51 %	Slow charging via VRFB, fast discharging via SC *OR* vice versa
Pathway 3	43 %	Fast charging via SC, intermediate storage in VRFB, fast discharging via SC
Pathway 4	79 %	Fast charging and discharging via SC, no use of VRFB

[1] Values assessed in HyFlow WP1 and 2, efficiency of the developed high power VRFB [18].
[2] Value provided by manufacturer.
[3] Adopted from [19].

2.1.2.5. EoL phase of HESS. For the EoL phase, it was assumed that the HESS would be transported to a recycling facility and mechanically dismantled. Subsequently, its components respectively materials would be recycled, whenever feasible. The applied recycling and disposal pathways for individual components, including LCI tables, are indicated in the SI. Following Weber et al. [21], a high recycling efficiency of 95 wt% was assumed for all metal parts that can be easily separated from the system during dismantling; residual metal was modeled to be landfilled. Metal recycling was mainly set up following Quéheille et al. [68]. For all plastic components, including membranes, electrodes and bipolar plates, waste incineration with energy recovery was chosen, which was also assumed by Weber et al. for VRFBs [21]. For lithium ion batteries (LIBs), recycling of plastic components is not yet state-of-the-art, but plastic is usually decomposed during thermal pretreatment (pyrolysis) in the battery EoL process [69]. However, with respect to circular economy, recycling of HESS plastic components should be assessed in the future. There is also ongoing research in recycling of special plastic products such as Nafion® polymers [70–72] that are contained in the VRFB. However, due to reasons of complexity and data availability, plastic combustion was currently prioritized over recycling for the EoL LCA model in this study. The EoL phase of the HESS was assessed in four scenarios, with and without credits for recycled materials and recovered energy from waste combustion, as visualized in the SI (chapter 2.3).

2.1.3. Life cycle impact assessment and scenario development

Modeling and calculation of the LCIA was performed in the "LCA for Experts" 10.7 software [45]. For the LCIA the harmonized ReCiPe 2016 q(H) v1.1 methodology [73,74] was applied, transferring the results of the LCI analysis into 18 impact category indicators at midpoint. Moreover, the net primary energy demand (PED) of the HESS lifecycle was evaluated based on the cumulative energy approach and differentiating between PED from renewable (PEDn,r) and non-renewable sources (PEDn,nr) [75,76]. A complete list of all investigated indicators with their abbreviations and units is provided in the SI (chapter 3). Only the abbreviations of the indicators are used throughout this publication to improve readability.

The entire HESS lifecycle was assessed in 12 scenarios (Fig. 8), differing in the origin of the applied vanadium electrolyte and in the electricity source for charging of the HESS:

- Vanadium electrolyte:
  - o V_2O_5 I [21], primary (original allocation factors)
  - o V_2O_5 II [20], primary
  - o V_2O_5 III [49], secondary
  - o Recycled electrolyte (this study)

- Electricity sources:
  - o Conventional grid mix (European average)
  - o PV power (European average)
  - o Wind power (European average)

2.1.4. Sensitivity analysis

The effects of the alteration of the storage efficiency of the HESS were investigated through a sensitivity analysis, as this is the main parameter determining the environmental impacts of the HESS in its use phase. Its value was altered from 60 % to 45, 50, 55, 65, 70 and 75 %, while all other system parameters were left the same. This analysis was first performed on a HESS with primary V_2O_5 by Blume et al. [20] and the conventional European grid mix for charging. Subsequently, the analysis was repeated for a HESS with recycled vanadium electrolyte (this study) and PV.

2.2. Laboratory tests on vanadium electrolyte recycling

We developed and demonstrated a process on laboratory scale for recycling of waste vanadium electrolyte. Results of these tests served as input for our LCA.

Although numerous methods for the extraction of V_2O_5 from primary or secondary sources have been presented in literature, there is little research addressing the recovery of vanadium from spent electrolyte solution used in flow batteries, despite it being relatively easily accessible in dissolved form. Blume et al. [37] described several techniques to reprocess spent electrolyte, including, depending on the electrolyte's state, precipitation and re-dissolving, electrochemical removal of contaminants and chemical oxidation of organic pollutants. The method presented in our article involves the extraction of vanadyl cations (Vanadium(IV) oxide, VO^{2+}) from a waste electrolyte solution at pH ≈3 via a two-step liquid-liquid extraction process with di(2-ethylhexyl) phosphoric acid (DEHPA) into an organic solvent. The recycling process was tested in a laboratory setup. The schematic of the recycling process is visualized in Fig. 3. DEHPA with kerosene as organic solvent has been reported as a reliable extraction agent for leaching vanadium from aqueous sulfate solution [77,78]. It is also widely used as an extractant for uranium and other rare metals. The method has the advantage that it works practically independent of the EoL state, as the extraction process under the proposed conditions is selective enough not to leach major pollutants from the solution, making it a potentially cost-effective and sustainable approach. The leaching conditions were derived from the Oak-Ridge report by Blake et al. [79]. In the second step, vanadium was extracted back into the more acidic sulfuric acid (H_2SO_4) to directly produce a VRFB electrolyte precursor solution. The two extraction steps were repeated several times, until the desired vanadium concentration was reached in the extract. The pH was adjusted after every iteration. Prior to extraction, the waste solution was conditioned to reach the desired vanadium(IV) concentration and pH. The precursor that resulted from the extraction was post-treated by mixing with additives and adjusting the valency from 4 to 3.5, in this case, using electrolysis.

First, the capability of DEHPA as an extractant was investigated for iron (Fe(III)) and copper (Cu(II)) as typical contaminants, as well as vanadium(V), which could remain in the solution if overoxidized. Copper contamination from the current collectors (CCs) may occur through internal leaks or corrosion of the carbon monopolar plates and usually has severe consequences as it may cause complete failure of the battery system if not mitigated [80]. Iron may contaminate the system via the pump or some other instrument and has been reported to negatively impact the battery performance [81].

2.2.1. Experimental methods

Solvent extraction experiments were carried out in the laboratory according to the extraction procedure described above using separating funnels. H_2SO_4 solutions (pH = 2) were prepared with the respective metal ions and initial metal concentrations of 0.3 mol/l for the contaminants and 0.5 mol/l for the vanadium species. The pH of the solutions was adjusted to approximately 2 after each extraction step, by adding NaOH or ammonia (for Cu). The metal concentrations of the initial solution were measured after each extraction step. Vanadium contents were measured using potentiometric titration. Iron and copper concentrations were measured using UV–Vis spectrometry after treating the metals to form acetate and ammonia complexes, respectively.

A laboratory scale setup was constructed for extraction experiments. The setup is explained in greater detail in the SI. Two mixer-settlers were built using standard PVC piping parts and two mixers (“BOLA” 6 mm PTFE agitator, *Bohlender*, Germany; with motor “SBS-ER-3000”, *expondo*, Germany). Three “NRD-05” centrifugal pumps (*Iwaki*, Japan) were employed to pump the liquids through the extraction stages. For pH regulation, the process pH electrode “PL A-91” by *Xylem* (Germany) and a “FEM 1.09” diaphragm pump by *KNF* (Germany) were used to measure pH and to dose the caustic solution, respectively.

The steps to generate the recycled electrolyte solution are as follows:

1. Fill spent electrolyte (valency ≥3.5) in waste tank and add 30 wt% hydrogen peroxide (H_2O_2) solution to oxidize all vanadium to vanadium(IV). For all experiments, vanadium electrolyte solution by *GfE Metalle und Materialien* (Nürnberg, Germany) was used with an initial composition of 52.7 wt% vanadium(IV) and 47.3 wt% vanadium(III), a total vanadium concentration of 1.58 mol/l and approximately 2 mol/l H_2SO_4. (Electrolyte had not been used in a battery before, but was left untouched for several years, hence the slight shift in valency towards vanadium(IV).)
2. Add 1 M sodium hydroxide (NaOH) to set the pH to approximately 3.
3. Fill 4 M H_2SO_4 solution in product tank, 1 M NaOH solution in caustic tank.
4. Fill organic solvent with extraction agent to organic tank: 0.2 M DEHPA in kerosene (boiling range 200 to 260 °C)
5. Run extraction process until vanadium(IV) concentration in product reaches ≥1.6 mol/l.

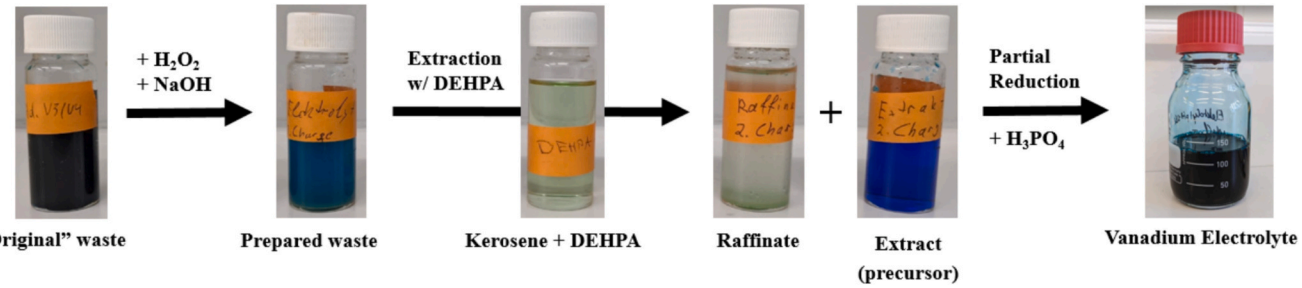

Fig. 3. Schematic of recycling process with the steps pre-processing, extraction and post-processing (arrows), and depiction of raw material, intermediate products and final product samples.

6. Using a single 40 cm^2 flow cell, charge extracted vanadium(IV) solution with constant current of 12.5 mA/cm^2 until cell voltage is ≥1.65 V and then with constant voltage of 1.65 V until current is ≤20 mA to generate vanadium(III) and vanadium(V) solution.
7. Mix vanadium(III) solution with extracted vanadium(IV) solution to reach the required valency of 3.5. (The vanadium(V) solution can be used instead of H_2O_2 in step 1 to oxidize spent electrolyte.)
8. Add phosphoric acid (H_3PO_4).

The experiments were performed with 6 l or 8.1 kg of electrolyte solution. Mass ratios of other starting materials and additives are listed in Table 4. Vanadium concentrations were evaluated using potentiometric titration. Concentrations of other elements were measured using inductively coupled plasma mass spectrometry (ICP-MS).

3. Results

At the beginning of this section, the results of the laboratory tests on waste vanadium electrolyte recycling are presented. Based on these results, we performed an LCA of the recycling process, which was eventually integrated in the LCA model of the HESS. Subsequently, the environmental impacts of the HESS in all lifecycle phases were assessed.

3.1. Laboratory tests on vanadium electrolyte recycling

The selectivity of DEHPA towards different vanadium species and major contaminants was investigated on a small laboratory scale. Fig. 4 shows the concentrations of different metal ions in the aqueous phase of the initial solution after each extraction step. It was demonstrated that DEHPA was able to extract vanadium(IV) from the sulfate solution most effectively. After three iterations, the concentration was close to the lower detection limit of the concentration measurement. Iron(III) could be extracted similarly well. However, copper was not easily leached from the solution, with two thirds remaining after 8 extraction cycles. Vanadium(V) was extracted poorly as well compared to V(IV). Therefore, the production of too much V(V) should be avoided during the initial oxidation step, in order not to waste too much vanadium during the extraction. In particular, the relatively poor selectivity towards copper is promising, as it can heavily disturb VRFB operation because it promotes hydrogen evolution in the vanadium electrolyte and hence causes irreversible capacity loss [80].

The extraction method was scaled up and automated using mixer-settlers. The resulting electrolyte solution was post-treated using an electrolysis cell for valence adjustment. Table 3 shows the vanadium concentrations in the original solution, the intermediate and finished products as well as the concentrations of other cations.

The extraction was stopped once the raffinate solution was virtually depleted of vanadium and the reaction stopped. The concentration in the extract was slightly higher than that of the initial waste solution. The subsequent increase in total vanadium concentration to 1.75 mol/l in the final product could be due to water crossing over the membrane as well as evaporation of water during the electrolysis process where the V(III) side was continuously purged with dry nitrogen. It is expected that the effect of evaporation will be reduced, if higher volumes of V(III) are processed.

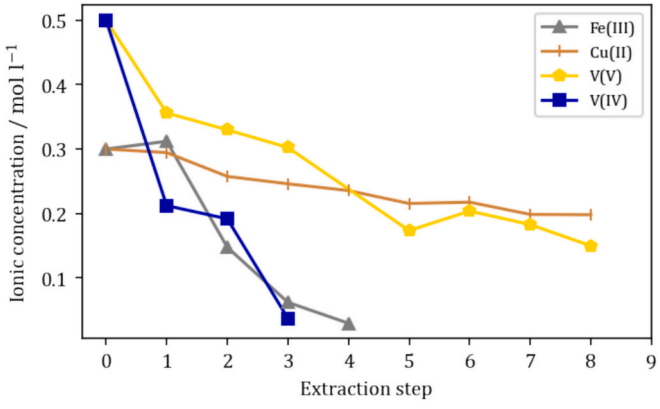

Fig. 4. Concentration gradients of various metal ions after extraction with DEHPA from sulphate medium.

Table 3
Vanadium concentrations and V(III) / V(IV) ratios before and after each recycling step.

Medium	Total V (mol/l)	V(III) (%)	V(IV) (%)
Initial waste solution	1.58	47.3	52.7
Pre-processed waste	0.33	3.3	96.7
Extract (precursor)	1.64	2.1	97.9
Raffinate (waste)	0.002	42	58
Electrolyte solution (final product)	1.75	49.3	50.7

The vanadium composition in the final product is suitable for direct use in a redox flow battery. If needed it can be diluted with water or sulfuric acid to achieve the desired concentration of vanadium species and free acid. Additives (e.g., phosphoric acid) can also be added as needed.

3.2. Environmental impacts of vanadium electrolyte

Based on the results of our laboratory tests we created an LCI of the recycling process of waste vanadium electrolyte on demonstrator scale as presented in Table 4. The process (reagent/component masses, energy demand, infrastructure, transport) was upscaled from a laboratory batch of a few liters to a batch of approximately 37 l recyclate, applying the LCA framework by Picchinno et al. [82] for the upscaling of chemical processes. The achieved recycling efficiency was 77 % by mass and 81.6 % by amount of vanadium, due to slightly differing vanadium concentrations in the feed material (1.6 mol/l) and the obtained recycled electrolyte in the laboratory tests (1.75 mol/l). For the LCI, the recycled electrolyte was modeled with a concentration of 1.6 mol/l. Further details on the compilation of this LCI are provided in the SI.

Fig. 5 displays the LCIA results of the production of 1 kg of recycled electrolyte with a vanadium concentration of 1.6 mol/l. The GWP of the recycling process accounted for 0.91 kg CO_2-eq/kg recycled electrolyte and the PED was 19.2 MJ/kg, with approximately 20 % of the PED originating from renewable sources. Sodium hydroxide (NaOH) was the main contributor in GWP, FFP, LOP, EOFP, HOFP and TAP and PED, while hydrogen peroxide (H_2O_2) was dominant in PMFP, WCP, FEP, IRP, MEP and ODP. The infrastructure for electrolyte recycling had the highest impacts in FETP, HTPc, HTPnc, METP, SOP and TETP; however, the latter results are associated with a relatively high degree of uncertainty, as the assessment of the infrastructure is based on a very rough approximation.

Fig. 6a and b compare the GWP and PED of the production of 1 kg of recycled electrolyte to 1 kg of electrolyte prepared with primary or secondary V_2O_5 from literature. LCIA results showed large differences, with the GWP of electrolyte production accounting for 0.9 to 11.4 CO_2-eq per kg of electrolyte and the PED ranging from (16) 19.2 to 98 MJ/kg of electrolyte. In addition to the original results for V_2O_5 I, we also display the results with allocation factors updated to current market prices. Details for all investigated midpoint category indicators can be found in the SI. Recycled electrolyte had a significantly lower GWP and PED than primary electrolyte modeled with V_2O_5 I (original) and V_2O_5 II and than electrolyte prepared with secondary V_2O_5 (V_2O_5 III). In addition, recycled electrolyte featured reduced impacts compared with the other datasets in 15 out of 17 other ReCiPe 2016 midpoint impact categories. Only in HTPc and LOP the recycled electrolyte had a higher impact than at least one other electrolyte. However, when comparing

Table 4
LCI for recycling of spent vanadium electrolyte.

Process	Ref. value	Unit	Used background process
Inputs			
Waste electrolyte (vanadium electrolyte for VRFB), 1.6 mol/l V	1.22	kg	Spent vanadium electrolyte from discharged VRFB
Hydrogen peroxide 30 wt%[1]	0.02	kg	SI
Sodium hydroxide (NaOH), 1 mol/l[1]	10.82	kg	SI
Sulfuric acid (H_2SO_4), 4 mol/l[1]	1.28	kg	SI
Phosphoric acid (H_3PO_4), 85 wt%[1]	0.009	kg	Market for phosphoric acid, industrial grade, without water, in 85 % solution state, ecoinvent 3.8, GLO
Di-(2-ethylhexyl) phosphoric acid (DEHPA)[1,2]	0.065	kg	SI
Kerosene[2]	0.83	kg	Market for kerosene, ecoinvent 3.8, Europe without CH
Electricity (pumping, stirring, charging, control system)	0.059[3]	kWh	SI
Water, deionized	0.065	kg	RER: Water (desalinated; deionized) Sphera
Infrastructure	4E-10	items	Market for chemical factory, organics, ecoinvent 3.8, GLO; factory with output of 50,000 t/a and a lifetime of 50 yrs
Transport, lorry	0.73	t.km	= transport of waste electrolyte to recycling facility, assumed transport distance 600 km by lorry [21]; Lorry transport incl. fuel, Euro 0–6 mix, 22 t total weight, 17.3 t max payload, RER, Sphera
Outputs			
Recycled vanadium electrolyte for VRFB, 1.6 mol/l V	1	kg	
DEHPA (Di-(2-ethylhexyl)phosphoric acid)	0.064	kg	Reused, loop to process input
Kerosene	0.81	kg	Reused, loop to process input
Raffinate (waste water)	12.43	kg	To waste water treatment: Waste water treatment (slightly organic and inorganic contaminated), EU-27, Sphera

[1] Transport of these substances already included in respective processes.
[2] Reused, loop to process input; losses of 3 wt% to raffinate assumed.
[3] Upscaled from lab-scale to batch of 37 l recyclate, following scale-up framework of [82].

the GWP and PED of recycled electrolyte to primary V_2O_5 I modeled with updated allocation factors, the picture was no longer so clear. This demonstrates the importance of having standardized, precise and freely usable LCI datasets available for primary V_2O_5 production, to be able to demonstrate the real benefits of the application of recycled/secondary compared to primary vanadium electrolyte.

We also performed a closer analysis of the environmental impacts of vanadium electrolyte prepared with the three selected V_2O_5 datasets from literature (chapter 2.1.3). Corresponding graphs are provided in the SI. It was observed that V_2O_5, regardless of the selected dataset, had the strongest impact on electrolyte production in most indicators, including GWP and PED. It should also be noted that V_2O_5 from the two primary sources had a high impact on SOP ($\geq$ 97 %), as expected with regard to its CRM status. However, in the indicators FETP, HTPc and METP the electrolyte component sulfuric acid was dominant for the two primary sources. Phosphoric acid only caused a significant contribution to the electrolyte's impact in HTPc and electricity in PEDr,n.

3.3. Environmental impacts of HESS production, use and EoL

This section presents the LCIA results for the production of all main HESS components, as well as for the use and EoL phases of the HESS. The entire HESS lifecycle was assessed in twelve scenarios, as visualized in section 3.3.6 . Environmental hotspots were outlined.

3.3.1. Production phase of VRFB

Environmental impacts of VRFB production in several scenarios are displayed in the SI. Vanadium electrolyte caused the highest share of the total environmental impacts of VRFB production in almost all scenarios and indicators, including GWP and PED. The only exceptions were HTPc in the primary and recycling scenarios, and SOP in the recycling scenario, where the VRFB-periphery was the dominant component. When comparing all VRFB scenarios, the primary dataset V_2O_5 II led to the highest overall impacts for the VRFB production in 10 out of 18 indicators – including GWP, and regarding PED. In WCP, FETP, HTPc, LOP, METP and MEP the secondary dataset V_2O_5 III showed the highest impacts. The VRFB modeled with recycled electrolyte featured the lowest impacts in 17 out of 18 impact indicators, with the only exceptions of HTPc, where the primary datasets V_2O_5 I and V_2O_5 II led to slightly lower results and LOP, where the primary dataset V_2O_5 I led to a slightly lower result. Even if originating from a secondary source, V_2O_5 III showed higher results in 11 indicators and regarding PED compared to the primary dataset V_2O_5 I. The VRFBs modeled with primary V_2O_5 datasets (V_2O_5 I and II) showed large differences, even with both of them describing the same mining process in South Africa. In addition, one has to keep in mind that results for V_2O_5 I would even be lower, when using current allocation factors. The GWP for the production of the VRFB in four scenarios ranged from 0.03 to 0.26 kg CO_2-eq/kWh, while the PED accounted for 0.63 to 4.57 MJ/kWh. These values demonstrate the wide range of possible LCIA results for the VRFB production, depending on the selection of V_2O_5 datasets respectively the application of primary or recycled electrolyte. However, the electrolyte remains the main contributor in most categories and scenarios.

3.3.2. Production phase of SC, DC-DC converters and periphery

The SC was evaluated using primary or recycled nickel for the CCs of the AC electrodes. The GWP of the SC production accounted for 6.7E-04 to 1.1E-03 kg CO_2-eq/kWh, while the PED ranged from 1.4E-02 to 2.6E-02 MJ/kWh. The electrodes – whether containing recycled or primary nickel – were the main contributors to environmental impacts in almost all impact indicators. The only exception was LOP, where nickel-coated copper connectors were dominant in the recycling case. Also regarding PED the electrodes were dominant. Using recycled nickel for CCs of the AC electrodes reduced the environmental impacts of the SC production in all investigated indicators and also decreased its PED. The GWP of the DC-DC converter production accounted for 5.5E-03 kg CO_2-eq/kWh and the PED was 8.9E-02 MJ/kWh. The inductors caused the highest impacts on converter production in most indicators, followed by the printed wiring boards, which were dominant in four indicators. Only for ODP, nylon came in second place after the inductors. Regarding the HESS periphery (PCS, wiring and containers), the production of the steel containers was dominant in all investigated impact categories and also for PED.

3.3.3. Production phase of entire HESS

Fig. 7a and b present the GWP and PED for the production of the entire HESS in several scenarios, as schematized in the SI. The GWP accounted for 0.05 to 0.28 kg CO2-eq/kWh and the PED ranged from 0.95 to 4.88 MJ/kWh, with the highest impacts on GWP and PED caused by the VRFB and its electrolyte. The VRFB was also dominant in most other indicators and scenarios. However, this was not true for FETP, HTPnc, METP and TETP, with the converters and inverter being the major contributors, and also not for HTPc, with the periphery causing the highest impact. The SC only had a minor impact on all impact

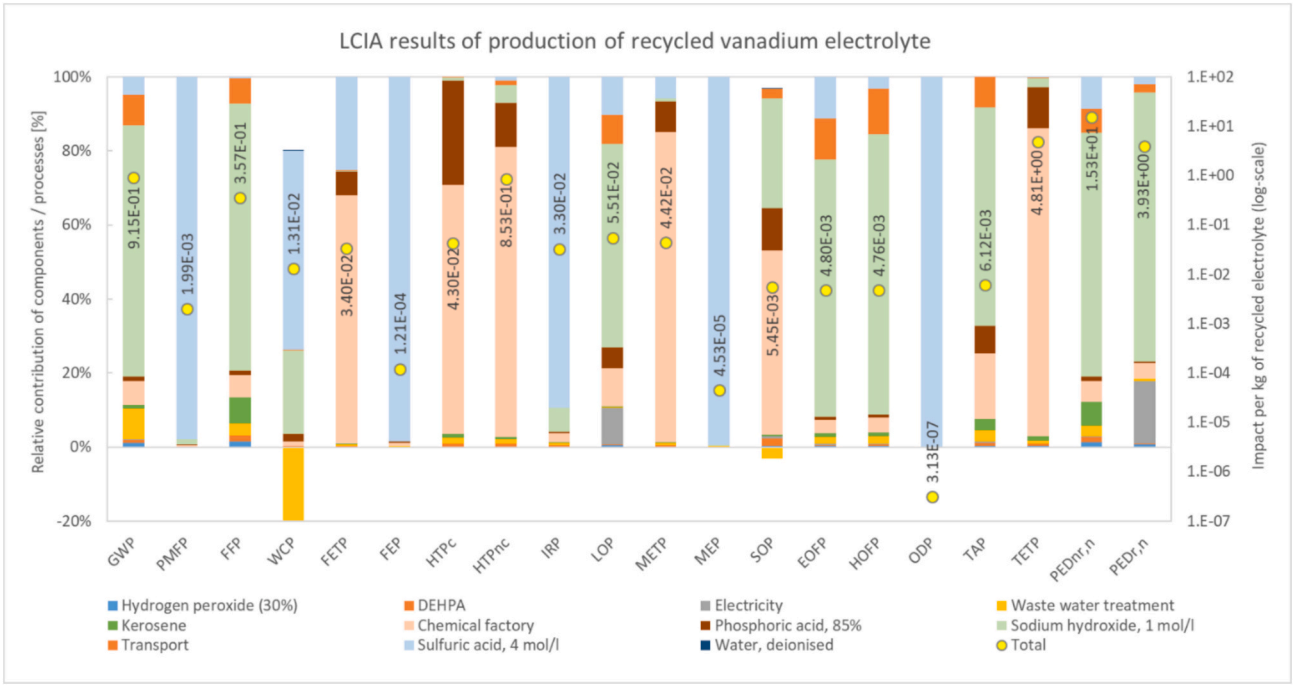

Fig. 5. Environmental impacts of production of 1 kg recycled vanadium electrolyte.

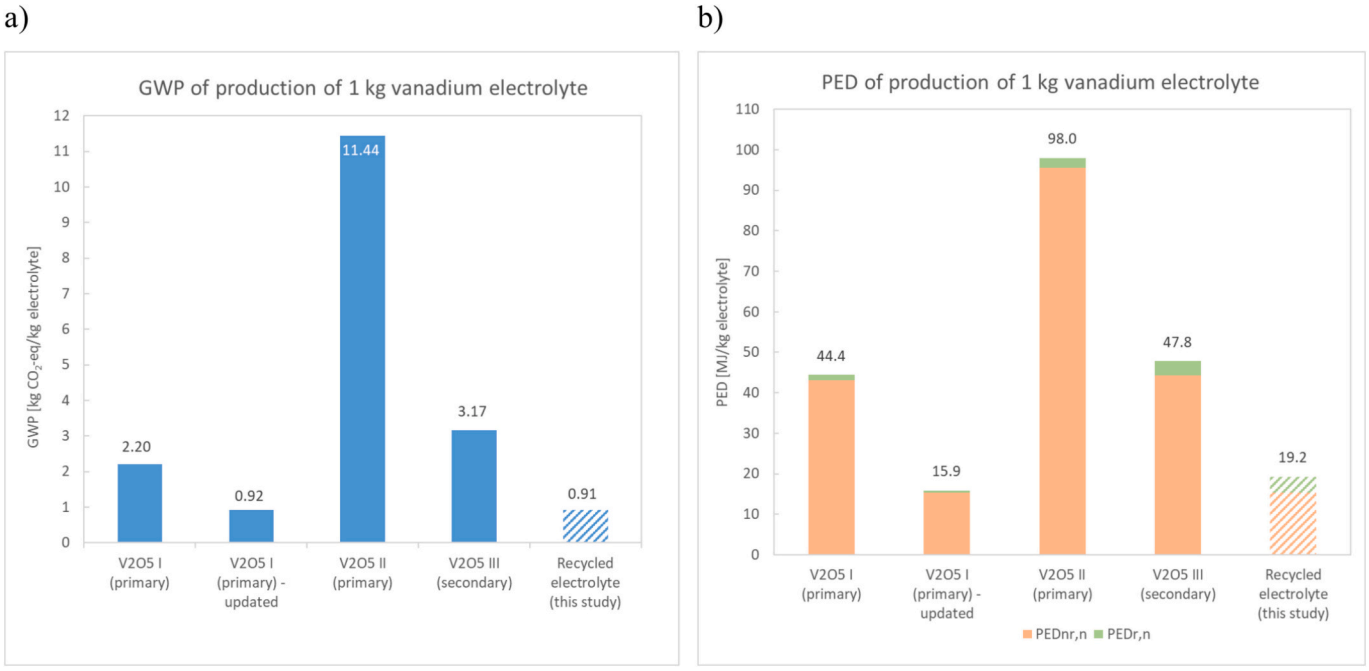

Fig. 6. a) GWP and b) PED of production of 1 kg vanadium electrolyte (V_2O_5 I (primary – updated) = value with updated allocation factors).

categories and on PED, causing for example only up to 2 % of the total GWP. Therefore, we decided not to consider the recycled-nickel SC in the HESS lifecycle scenarios, as this would only have a negligible influence on the overall LCIA results. Converters and inverter contributed up to 25 % to the total GWP of the HESS production phase.

3.3.4. *Use phase*

When charging the HESS with a conventional European grid mix, the electricity losses caused the majority of environmental impacts in 12 out of 18 indicators, including GWP. The GWP of the HESS use phase ranged from 0.01 to 0.20 kg CO2-eq/kWh, while the PED accounted for 6 to 14 MJ/kWh. As expected, the absolute impacts of the use phase were generally lower when the HESS was charged with renewables than with a conventional grid mix; this was true for example for GWP. However, in FETP, FEP, HTPc, HTPnc, METP, SOP and TETP only minor differences between electricity sources could be observed. In these category indicators the inverter exchange was dominant irrespective of the applied electricity source, except for SOP, which showed an equal share between electricity losses and inverter exchange. In ODP the VRFB stack exchange had the highest relative impact when charging the HESS with renewables. Also regarding PED, the electricity losses were the dominant contributors, with higher impacts for PV and wind. The SC

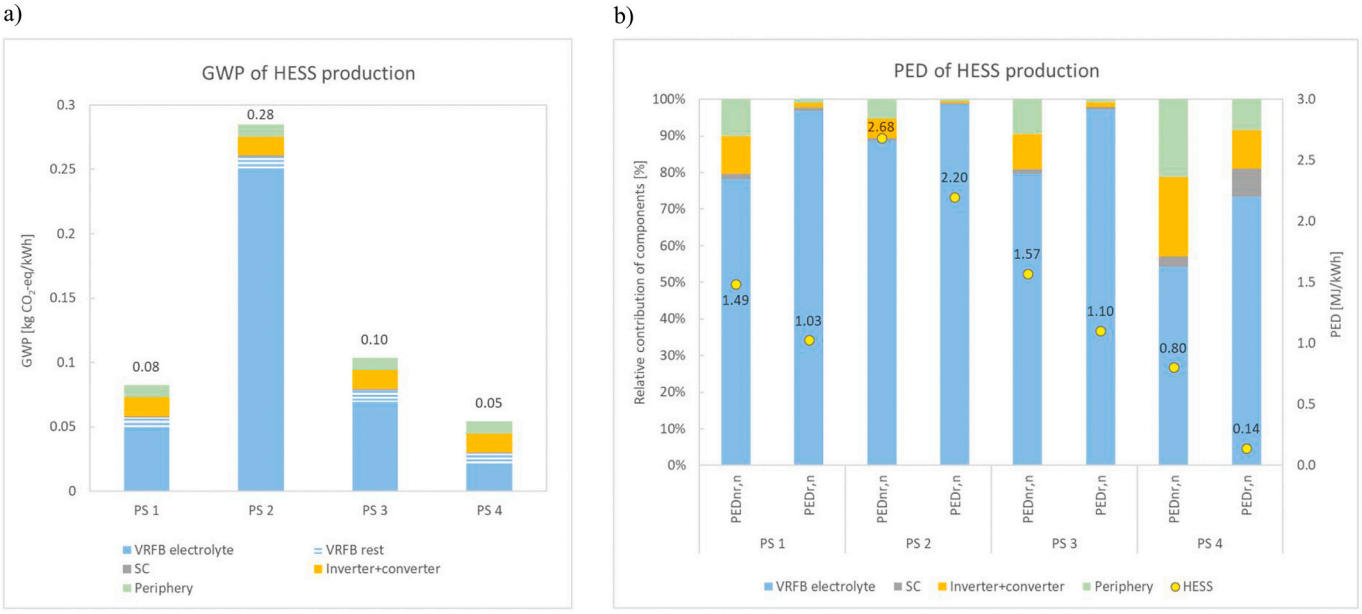

Fig. 7. a) GWP and b) PED of HESS production.

exchange only played a minor role in most scenarios and categories. To sum up, the choice of electricity source had a major impact on the overall LCIA results of the HESS use phase in many categories. This was for example also observed by Weber et al. [21]. In addition, the exchange of the inverter strongly influenced a number of impact indicators. For the lifetime of the inverter, a value of 10 years, hence one exchange within the operational time of the HESS was adopted from another publication [21], whereas for the converters the manufacturer estimated a much longer lifetime of over 50 years. Depending on the actual lifetime of the inverter, LCIA results of the use phase of the HESS specifically for FETP, FEP, HTPc, HTPnc, METP and TETP can vary strongly, while the changes in GWP or PED would be smaller. Graphs indicating all LCIA results for the use phase are provided in the SI.

3.3.5. *End-of-life phase*

The GWP of the EoL phase without credits accounted for 0.02 kg CO_2-eq/kWh, while the GWP with credits ranged from −0.19 to 0.01 kg CO_2-eq/kWh. The PED without credits accounted for 0.38 MJ/kWh, while the PED with credits ranged from -3.36 to 0.19 MJ/kWh. The PED mainly originated from non-renewable sources. Regarding expenditures and credits, the recycling process of vanadium electrolyte was dominant in most indicators, including GWP and PED. Only in FETP, HTPc, HTPnc, METP and TETP other processes clearly caused higher impacts. Further details are provided in the SI.

3.3.6. *Entire HESS lifecycle*

Fig. 9 presents the GWP of the entire lifecycle of the HESS in twelve scenarios, as schematized in Fig. 8. In 9 out of 12 scenarios the production phase was the dominant lifecycle phase regarding GWP (48–86 %). Moreover, the **vanadium electrolyte** was the main contributor to the production phase of the entire HESS in most scenarios (58–88 %), except for those modeled with recycled electrolyte (HESS 10, 11 and 12) (37 %). In scenarios HESS 1, 7 and 10, which were evaluated with the conventional European grid mix for charging of the HESS, the use phase caused the highest GWP impact (63–73 %). In scenario HESS 4, which was also modeled with the conventional European grid mix, the share of the use phase in the entire HESS lifecycle was 41 %.

The use phase was mainly shaped by the **electricity losses during charging and discharging** (60–94 %), except for HESS 3, 6, 9 and 12, which were modeled with wind power (39 %). The GWP for the entire HESS lifecycle ranged from 0.10 to 0.53 kg CO_2-eq/kWh. The GWP of scenarios calculated with the primary V_2O_5 II dataset was generally higher than that of scenarios calculated with V_2O_5 I and V_2O_5 III, as well as with recycled electrolyte (cf. chapter 2.1.3). The highest lifetime GWP was found for HESS 4, which was modeled with primary V_2O_5 by Blume et al. [20] and with a conventional European grid mix for charging. The lowest lifetime GWP resulted from HESS 11 and 12, which were modeled with recycled vanadium electrolyte and charged with PV or wind power. GWP hotspots in the lifecycle of the HESS are visualized in

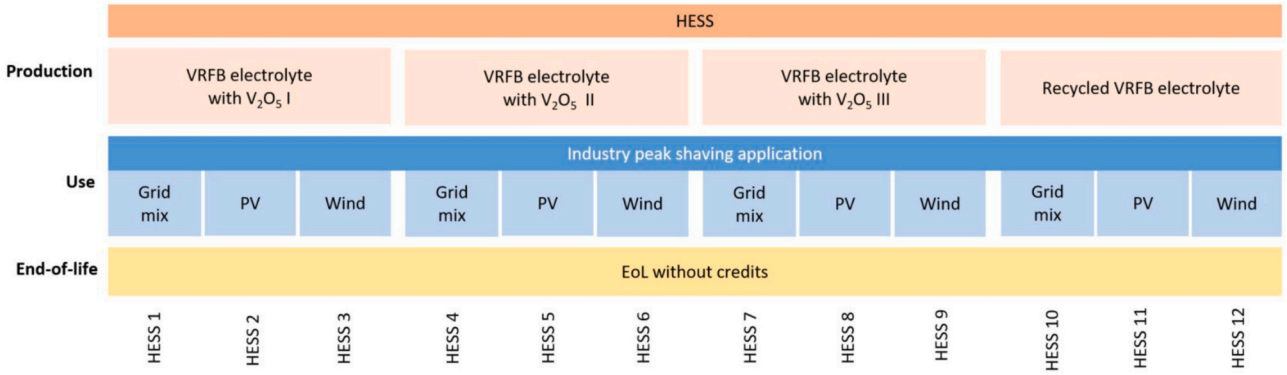

Fig. 8. Scenarios for entire lifecycle of HESS (chapter 2.1.3).

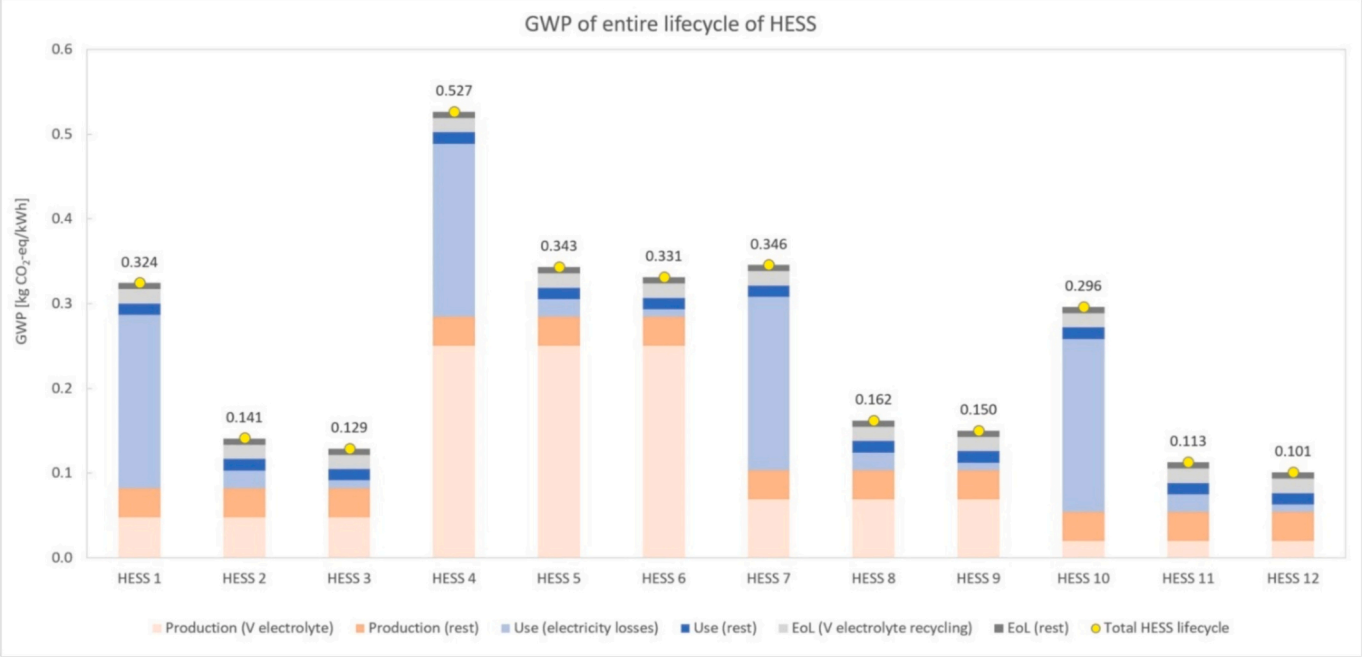

Fig. 9. GWP of entire HESS lifecycle in twelve scenarios.

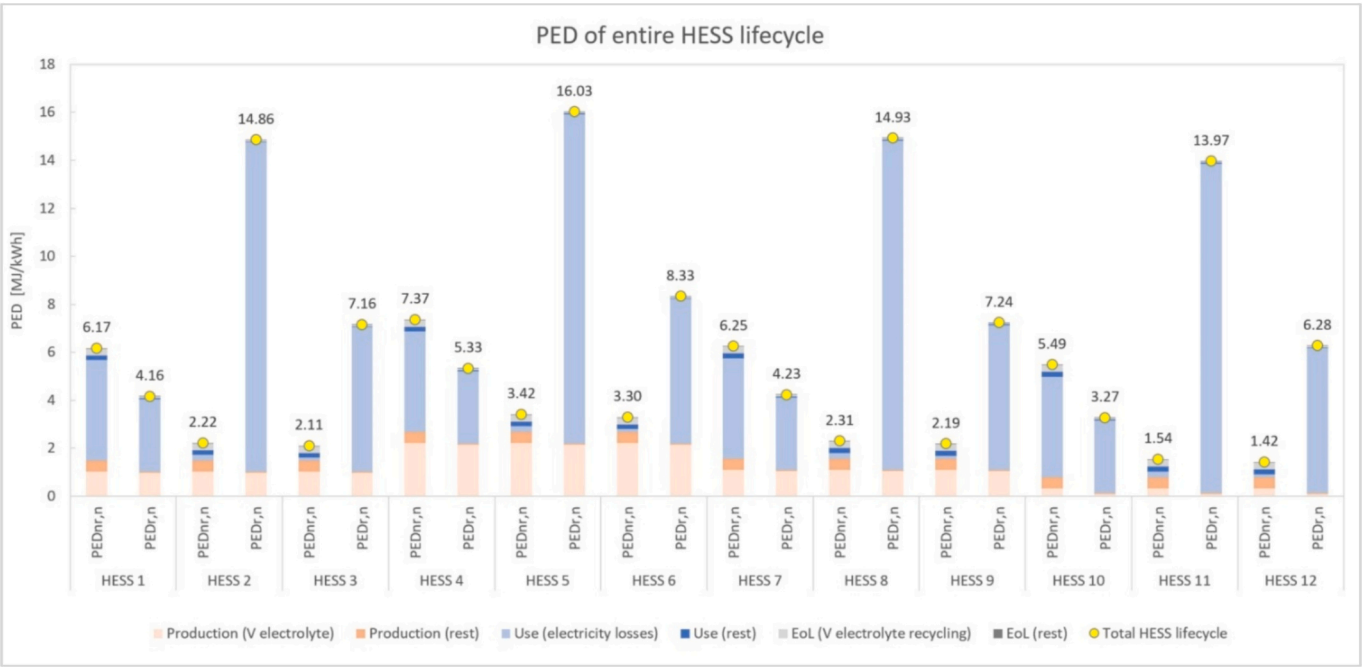

Fig. 10. PED of entire HESS lifecycle.

Table 5, with hotspot factors indicated.

When investigating the results for other impact indicators, which are presented in the SI, the production phase of the HESS was the dominant lifecycle phase in most scenarios and indicators, with only a few exceptions.

The PED of the HESS lifecycle (Fig. 10) ranged from 7.7 to 19.4 MJ/kWh, which, again, underlines the wide range of possible results depending on scenario parameters. In contrary to the GWP, the main contributors to PED over all scenarios were the electricity losses that occur during charging and discharging in the use phase of 20 years. In second place was the production of vanadium electrolyte. The highest PED could be observed in the PV charging scenarios (HESS 2, 5, 8 and 11), with however, the majority of the PED originating from renewable sources.

4. Discussion

In this section, results of our study are compared to LCA studies from the existing literature on VRFBs and LIBs. In a sensitivity analysis, the effects of an alteration of the HESS storage efficiency on its environmental performance were evaluated. Subsequently, data quality and uncertainty, as well as limitations of our study, were discussed.

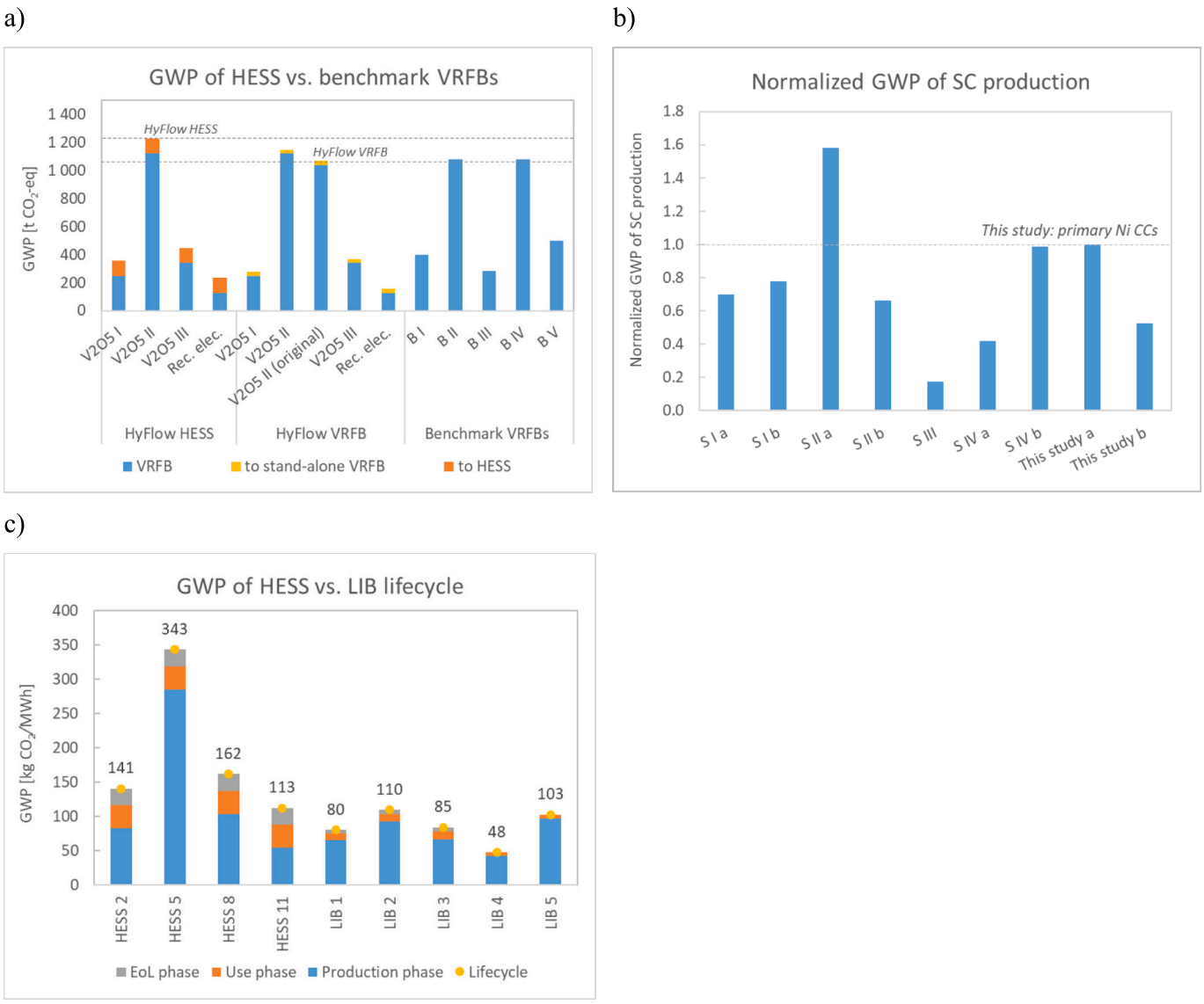

Fig. 11. a) GWP of production of 1 unit of industrial scale HESS and stand-alone VRFB (this study), compared to five benchmark VRFBs (original GWP results extrapolated); b) GWP of production of SC (this study) compared to benchmark SCs; c) GWP of HESS compared to LIB lifecycle, LIB 1 = NMC [19], LIB 2 = LTO [21], LIB 3 = LTO, partly recycled materials [21], LIB 4* = NCA-C [86], LIB 5* = NCO-LTO [86]; *only production and use phase.

4.1. Benchmarking

Fig. 11a compares the GWP of the production of an industrial scale stand-alone VRFB, based on data from this study, to the industrial scale HESS and benchmark VRFBs. The results include the required AC-DC inverter- and DC-DC converter-sizes, as well as the PCS, but do not include housing or foundations. The GWP of the HESS production was 7 to 53 % higher compared to that of the stand-alone HyFlow VRFB. The additional GWP expenses of the "high-power function" of the HESS compared to the stand-alone VRFB are caused by the fact that the HESS requires two DC-DC converters, a larger AC-DC inverter and a SC. The DC-DC converters and the larger AC-DC inverter cause the major part of these additional GWP expenses, whereas the SC itself only plays a minor role. It must be noted that VRFBs and the HESS are not directly comparable, due to their differing fields of application and overall energy efficiencies.

Five VRFBs from literature were selected for benchmarking (Table 6). These studies assessed VRFBs of different sizes and applied strongly differing numbers of dis−/charging cycles. Therefore, GWP results as indicated in Table 6, could not be directly compared neither to each other, nor to the HyFlow stand-alone VRFB. Hence, to achieve better comparability, the GWP results for the production of the benchmark VRFBs were extrapolated based on HyFlow parameters (net storage capacity and net power); extrapolated values are presented in Fig. 11a. It must be emphasized that this comparison is based on approximations.

B I, B III and B V were modeled with the V_2O_5 I dataset, whereas B II and B IV applied V_2O_5 II. The HyFlow stand-alone VRFB with V_2O_5 II showed a slightly higher GWP than B II and B IV, because our remodeling of the V_2O_5 II dataset resulted in a higher GWP per kg of V_2O_5 than the original value published by Blume et al. [20]. This can be explained by different used LCI database versions and the fact that Blume did not indicate the exact used background LCI datasets that they used for their V_2O_5 model. Blume also contributed to the LCA of B IV, hence being able to use the original V_2O_5 model. Therefore, we also approximated our VRFB using the original Blume V_2O_5 GWP value. In this case, our VRFB exhibited a slightly lower GWP than the benchmark VRFBs; however, this difference is not significant owing to the approximated benchmark value. B I and B IV used different electrolyte chemistries than the one applied by B III and in our study and additionally, B

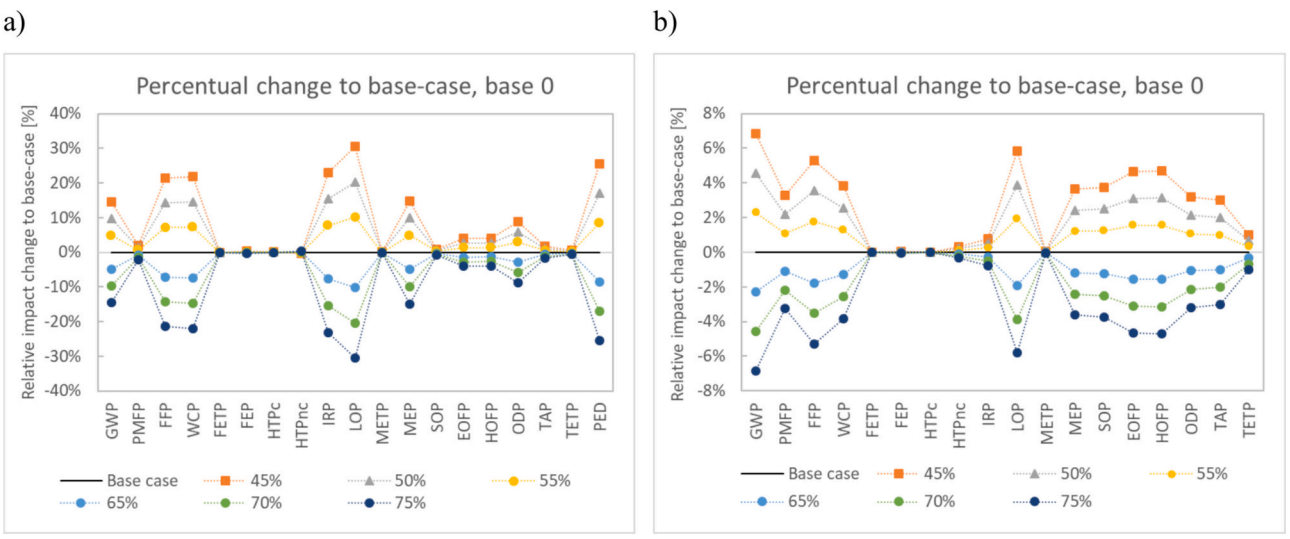

Fig. 12. Sensitivity analysis of HESS lifecycle, altering HESS storage efficiency, HESS production with a) primary V_2O_5 [20], charging with conventional European grid mix (PED is not displayed for better visibility), and with b) recycled electrolyte (this study), charging with PV; connecting lines only serve for better visibility.

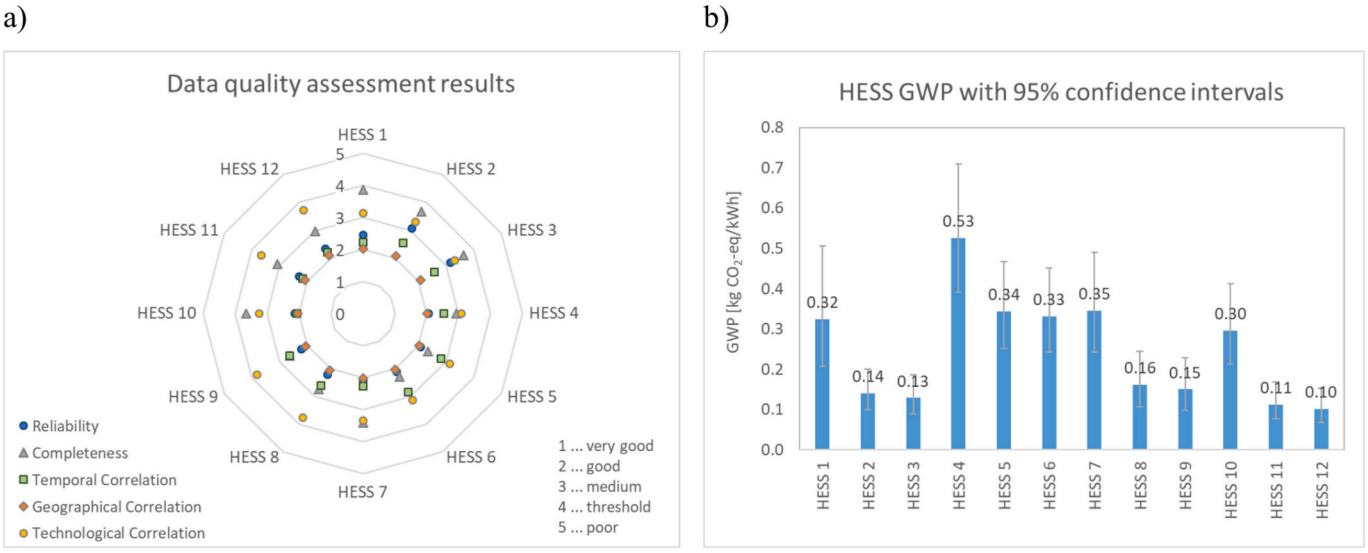

Fig. 13. a) Data quality assessment results (pedigree scores) for all 12 HESS lifecycle scenarios (1 = highest, 5 = lowest data quality); b) GWP per kWh of HESS production, use and EoL, indicating 95 % confidence intervals from uncertainty analysis, based on σ^2_{total} (lognormal distribution).

IV updated the V_2O_5 I dataset (economic allocation with more recent market prices for by-products). This impedes the comparability between VRFBs modeled with V_2O_5 I.

A comparison of the SC presented in this study to benchmark SCs is provided in Fig. 11b. S I [26] is an AC/acetonitrile SC with partly recycled (a) or only primary AC and aluminum (b). S II [25] is an SC with acetonitrile-based electrolyte and either graphene (a) or AC (b) electrodes. S III [23] features AC electrodes from hard coal and an acetonitrile-based electrolyte, and S IV contains AC from coconut shells with either an ionic liquid (MPPyFSI) (a) or 1 M H_2SO_4 as electrolyte. S I and S II are based on the same 5F/0.005 Wh SC cells [85]. In contrary to all benchmark SCs, our SC features an aqueous electrolyte. The GWP per kWh of storage capacity of our SC lies within the range of the benchmark SCs. The highest GWP was caused by the graphene SC (S II a), which can be attributed to its higher specific capacitance and higher energy consumption for production [23]. Different used functional units, SC chemistries and sizes render the comparability of these studies challenging.

Due to their overlapping, yet not identical, fields of application, a comparison of the HESS to LIBs for stationary use regarding their environmental performance is of interest. Three publications on the LCA of stationary LIBs [19,21,86], covering different LIB types, were selected for benchmarking as indicated in Fig. 11c. To render LCIA results comparable, we applied the number of charge−/discharge cycles of our study to the selected LIBs and used the same emission factors for PV. The presented values in Fig. 11c include the production, use and EoL phases (without credits).

It is important to note that our EoL model is not directly comparable to those of the cited LIB studies: They finished after dismantling of the HESS, while we also accounted for further recycling steps, until availability of a recycled product that can substitute a primary product. Hence, our EoL results were higher. Moreover, for LIB 4 and LIB 5 no GWP values for the EoL phase were available.

The LIB LCA studies cited here do not report a wide range of midpoint impact category indicators and in some cases are even limited to GWP. For the use phase, Le Varlet et al. [86] did not consider an

Table 5
GWP hotspots in HESS lifecycle, indicating hotspot factors.

	HESS production						HESS use	HES EoL				
	VRFB electrolyte	VRFB rest	SC	Inverter	Converters	HESS periphery	Hess use	VRFB electrolyte	VRFB rest	SC	Converter + inverter	HESS periphery
HESS 1	15%	3%	0%	3%	2%	3%	67%	5%	2%	0%	0%	0%
HESS 2	34%	7%	1%	6%	4%	7%	24%	12%	4%	0%	1%	1%
HESS 3	37%	7%	1%	7%	4%	7%	17%	13%	4%	0%	1%	1%
HESS 4	48%	2%	0%	2%	1%	2%	41%	3%	1%	0%	0%	0%
HESS 5	73%	3%	0%	3%	1%	3%	10%	5%	2%	0%	0%	0%
HESS 6	76%	3%	0%	3%	1%	3%	7%	5%	2%	0%	0%	0%
HESS 7	20%	3%	0%	3%	2%	3%	63%	5%	2%	0%	0%	0%
HESS 8	43%	6%	1%	6%	3%	6%	21%	11%	3%	0%	1%	1%
HESS 9	46%	6%	1%	6%	4%	6%	15%	11%	3%	0%	1%	1%
HESS 10	7%	3%	0%	3%	2%	3%	73%	6%	2%	0%	0%	0%
HESS 11	18%	8%	1%	9%	4%	9%	30%	15%	5%	0%	1%	1%
HESS 12	20%	9%	1%	10%	4%	10%	22%	17%	5%	0%	1%	1%

Table 6
Specifications and GWP of production phase of HyFlow VRFB and benchmark VRFBs.

ID	Power / storage capacity	No. of applied cycles [−]	$GWP_{production}$ [kg CO_2-eq/kWh]
B I [21]	723 kW_{net} / 6,000 kWh_{net}	8,176	0.038
B II [20]	1,000 kW_{net} / 8,000 kWh_{net}	20,000	0.036
B III [83]	500 kW_{net} / 2,000 kWh_{net}	7,300	0.028
B IV [84]	500 kW_{net} / 2,000 kWh_{net}	20,000	0.04
B V [19]	- / 30 kWh_{net}	6,000	0.051
VRFB (this study)		5,143	0.26

exchange of components in 20 years of operation of LIB 4 and LIB 5. Weber et al. [21] accounted for a partly exchange of cells after 10 years, which however, only resulted in a minor contribution to the environmental impacts of the use phase (LIB 2, LIB 3). Da Silva Lima et al. [19] assumed a lifetime of the LIB of 10 years, hence one complete exchange in 20 years, which they already accounted for in the production phase (LIB 1). When taking a closer look at the production phase of the HESS and the LIBs in Fig. 11c, it got obvious that HESS 3, which was modeled with V_2O_5 II [20], showed significantly higher results than the cited LIBs in GWP and all other indicators. The HESS features a lower total efficiency than LIBs and thus caused higher losses and higher associated environmental impacts in the use phase. Hence, the HESS with this primary electrolyte did not appear to be competitive with LIBs in terms of environmental impacts. On the other hand, the HESS with recycled electrolyte (HESS 11) featured a comparable lifecycle GWP as LIBs and also exhibited a better or at least similar performance in terms of PMFP, TAP and SOP (cf. SI). In HTP (sum of HTPc and HTPnc) the LIBs showed lower indicator values than all HESS scenarios. The lower PED of the cited LIB may be due to the higher total efficiency of LIBs [11]. In their review paper, Ebner et al. [11] stated that the comparison between VRFBs and LIBs in other studies often was not unambiguous, with rather similar results regarding GWP and a better performance by the VRFB regarding HTP. In our case, the HESS performed worse than the LIBs in the latter category, which may be due to its larger inverter and the two additional converters compared to a stand-alone VRFB. There is no distinct winner over all impact categories. It should be emphasized that this comparison is not exhaustive, owing to the large number of different LIB types and the fast ongoing development in this field. However, we may conclude that the HESS, if produced with recycled electrolyte and charged with renewables, could be a real competitor in terms of GWP to LIBs for large-scale stationary energy storage.

4.2. Sensitivity analysis

Fig. 12a and b presents the results of the sensitivity analyses of the HESS parameter “storage efficiency”. The first analysis, as depicted in Fig. 12a, is based on a HESS modeled with primary V_2O_5 by Blume et al. [20] and with the conventional European grid mix for charging. An increase of the storage efficiency from 60 to 70 % would decrease the GWP by approximately 10 %. The alteration of the storage capacity had a strong impact on 7 out of 18 ReCiPe 2016 category indicators (±9 to ±30 %), as well as on the PED (±25 %). Other indicators only showed minor reactions.

The same sensitivity analysis was repeated for a HESS produced with recycled electrolyte (this study), and charged with PV. Results of the second sensitivity analysis are displayed in Fig. 12b. In this case, the GWP was only reduced by approximately 4.6 % when increasing the efficiency from 60 % to 70 %, while the PED decreased by 22 %.

These sensitivity analyses demonstrated that improving the storage efficiency enhanced the environmental performance of the HESS lifecycle across many impact categories; however, these positive effects were less pronounced for a HESS produced with recycled electrolyte and charged with electricity from renewable sources. Moreover, possible expenditures of future optimization measures (impacts of new or additional required materials, energy etc.) were not yet included in this calculation.

4.3. Data quality and uncertainty

In this study, data uncertainty was addressed using multiple approaches, including scenario analysis, sensitivity analysis, and

qualitative assessment of LCI data quality and uncertainty. All three approaches concentrated on primary and secondary data responsible for the GWP hotspots in the HESS lifecycle. Our LCA approach surely could be determined as pLCA, for which research is ongoing on how to treat uncertainty [87]. Šimaitis et al. [88] highlight relevant and groundbreaking works, such as (10–16), which are all heavily scenario-based. Bisinella et al. [89] emphasize that the scenarios should be developed in close collaboration with experts.

This study aimed at integrating the best available LCI data. In case of the foreground HESS data this meant that we applied primary manufacturer data for the main components, even if upscaled. The only exceptions were the AC-DC inverter, which had to be approximated from a readily-available ecoinvent dataset for a PV inverter, and the HESS periphery. However, for reasons of completeness, we chose to include these components in the LCA of the HESS.

Regarding the applied background LCI datasets, the following must be noted: For many products or processes more than one LCI background dataset is available in commercial databases or in the existing literature, often providing different LCIA results due to differing material parameters, production routes, geographical location etc. Hence, significant effort went into selecting the most suitable datasets that (1) best describe the respective product or process, (2) are valid from a temporal and geographic perspective and (3) originate from reliable sources, such as peer-reviewed literature or renowned LCA databases.

To assess the overall data quality and uncertainty of our LCA study, we applied a simplified qualitative approach following Weidema and Wesnæs [90]. This five-dimensional methodology was further advanced by ecoinvent [91–93]. A description of the entire assessment process, as well as the intermediate results, are provided in the SI.

The first step of this methodology was data quality assessment through a pedigree matrix, where each phase of the HESS lifecycle and the main components were evaluated based on five data quality indicators: *reliability*, *completeness*, *temporal correlation*, *geographic correlation*, and *technological correlation*. The indicators were rated on a scale from 1 to 5, where 5 indicates lowest and 1 highest data quality. The pedigree scores of the HESS lifecycle phases accounted for the quality of the (1) *primary* LCI data for HESS production, use and EoL, and the quality of the (2) *most relevant background datasets* causing GWP hotspots in each lifecycle phase. The overall scenario scores for each indicator were then obtained by multiplying the pedigree scores of the single lifecycle phases or components by their GWP hotspot factors (Table 5), to give more weight to the main GWP contributors.

The pedigree scores for all 12 HESS lifecycle scenarios are shown in Fig. 13a. It is evident that the pedigree scores are generally higher for *technological correlation* than for the other indicators. This can be attributed to the fact that LCI foreground data for production of the HESS components were derived to a large extent from small-scale commercial or laboratory setups and upscaled to industrial size. Upscaling methodologies were applied in accordance with manufacturers respectively project partners; however, a certain deviation to real large-scale setups may persist. The *technological correlation* scores for HESS 8,9,11 and 12 were even lower, because, in these cases, LCI background data for vanadium production were derived from laboratory scale processes.

HESS 1–3 were rated with the highest scores in *completeness* and *reliability*, due to the used literature source for V_2O_5 production, where a problematic economic allocation of by-products was applied.

Medium to good ratings were achieved regarding *credibility* for HESS 4–12. We used LCI datasets originating from peer-reviewed publications and renowned commercial LCA databases, with the oldest *main* literature source dating back to 2018.

Data quality in this LCA study was mainly limited by data availability, for example by primary data currently only available at the laboratory scale or from smaller-scale commercial products. It would certainly be of advantage to verify the obtained results with data from real large-scale components or to approximate scaling effects in a future study.

To contextualize the results of this data quality assessment, it should be noted that none of the indicators across all scenarios were rated ≥ 4, a level we defined as acceptable. Moreover, a score of 1 (very good) is difficult to attain and is generally limited to independently-verified primary data from commercial applications of the corresponding scale or very recent peer-reviewed sources.

In the second step of the applied methodology, the obtained pedigree scores for each indicator were transferred to the variances (σ^2) of a lognormal distribution [92], which were used to calculate a total variance for each HESS lifecycle scenario [90]. Results for the HESS lifecycle GWP with upper and lower bounds of a 95 % confidence interval are displayed in Fig. 13b. The GWP of HESS 12 (recycled vanadium electrolyte, wind power) has a mean value of 0.10 kg CO_2-eq/kWh with its lower bound at 0.07 and its upper bound at 0.15 kg CO_2-eq/kWh. The confidence interval is smaller in this scenario than for HESS 3 (primary V_2O_5 [21], charged with wind power).

The results of uncertainty assessments for pLCA studies have to be interpreted with caution, as they can potentially mislead readers. Their interpretation also strongly depends on the goal of the LCA study: In case of the HESS, the identification of environmental hotspots in its lifecycle was of highest importance, as these findings can serve as a basis for further technological development and may help to define basic preconditions for technology deployment. However, if the exact LCIA results of the HESS are to be compared with those of other energy storage technologies, such as LIBs, and used to support decision-making between the two options, data uncertainty becomes a critical factor. A comparison between the HESS and LIBs is certainly of high interest for stakeholders, therefore we included it in the benchmarking section. However, owing to the diversity of LIB types, fast development in LIB technologies and data uncertainties on both sides, this comparison is not definite, exhaustive or suitable as a basis for decision making. This objective is beyond the scope of our study.

4.4. Further limitations and outlook

As already stated by Blume et al. [20] and He et al. [49], it is important to have standard and freely usable primary V_2O_5 datasets on regional and/or global levels at hand, specifically for the main vanadium-mining countries China, South Africa and Russia. This allows for a harmonization of LCIA results for VRFBs, for an evaluation of the benefits of recycled electrolyte and for benchmarking with other ESTs. Most primary datasets in the existing literature only describe gate-to-gate processes, hence ignoring important process steps. This is a flaw in our opinion, even if the main goal of some of these studies is the comparison of different gate-to-gate production routes. Moreover, a systematic assessment of currently available and possible future amounts and environmental impacts of secondary V_2O_5 in Europe would be of high interest for future research.

Further research is needed to improve and optimize the presented recycling process for spent vanadium electrolyte, especially regarding automated test plants. The recycling efficiency of 81.6 % by amount of vanadium was relatively low, most likely due to the vanadium remaining in the organic phase. Not all of this vanadium is lost, and it should be possible to recover it, if the organic solution is reused in a subsequent batch. However, this was not confirmed yet, as the focus was on the proof-of-concept. Hence fresh solutions were used for each experiment to begin from a defined starting point. Furthermore, a certain amount of vanadium could be in a different oxidation state (3 or 5), where it is more difficult to recover from the organic solution. This could only be overcome by setting the oxidation state in the pre-processing step with more precision. The long duration of the process can be overcome by scaling up and using multiple extraction stages. As of yet, not all steps were automated. For this study, valence adjustment required manual intervention. However, a corresponding reactor can be included in a recycling plant, either electrochemically with an electrolysis cell similar

to the one used in this study, or chemically, for example using organic oxidation agents in a continuous flow reactor, as described by [37] or [94]. Process simulation and further upscaling of the process to industrial scale should be targeted in future projects.

Our demonstrated recycling process represents a low level of technology readiness (TRL) and prospective LCA (pLCA) poses a number of challenges, owing to necessary approximations, unforeseeable future developments and possible technological changes. In our study, the LCA framework of Piccinno et al. [82] for the upscaling of chemical processes was applied to transfer LCI data from the laboratory scale recycling process to a larger scale. Nevertheless, this approach can only be a first approximation and special caution is required when interpreting the obtained results and comparing them with data from processes at higher technology readiness or even well-proven industrial processes. At an early stage of process development, the most sensible purpose of LCA usually is to identify environmental hotspots in the suggested process, which can serve as a basis for process improvement [95] and which was done in this study.

Most components of the vanadium electrolyte and the reagents used in the electrolyte recycling process are classified as hazardous under the UN's Globally Harmonized System (GHS) of Classification, Labelling and Packaging of Chemicals [96]. Substances holding this classification require a multitude of precautionary measures during manufacturing, transport, storage, use and disposal, to protect humans and the environment. The virgin and the waste vanadium electrolyte exhibit the most severe health and environmental hazards of all involved reagents. These include i.a. acute toxicity, cancerogenity, reprotoxicity, corrosivity and environmental hazards. The additional substances applied in the recycling process, although not holding a CMR (cancerogenic, mutagenic, reprotoxic) classification, add flammability and oxidizing effects to the list of hazards. The health and environmental risks associated with both the production and the recycling of vanadium electrolyte are not only relevant in the lab environment, but are also key elements that need to be taken into account in upscaling the recycling process. This usually increases the project's complexity and expenses. Recycled electrolyte, as demonstrated in this study, exhibited lower cradle-to-gate environmental impacts than electrolyte prepared with primary V_2O_5 II. However, it still would be worth evaluating the potential for substitution of hazardous substances, where possible. More information is provided in the SI.

5. Conclusions

This article reports on the LCA of a new HESS for stationary power storage that combines the advantages of a VRFB and a SC. The HESS was demonstrated on industrial scale and is able to simultaneously deliver high energy and high power (1,400 kWh / 900 kW). This LCA aimed to identify environmental hotspots in all lifecycle phases and to derive recommendations for an environmentally-friendly market deployment of this novel technology. The LCA of the HESS was performed for a real use case of consumption peak shaving in German industry over 20 years.

Foreground LCI data on the main HESS components, including used materials and their masses, were directly supplied by manufacturers. This enabled the generation of new inventories for the supercapacitor and the DC-DC converters, addressing data gaps in the existing literature. Furthermore, a large quantity of background LCI data, for example on the production of used materials or generation of consumed energy, had to be compiled. On the one hand, the HESS components contain a large number of materials, for some of which no readily available datasets exist in literature. New datasets had to be created, for example based on patents. On the other hand, for V_2O_5, the active component in the VRFB's electrolyte with significant environmental impacts, a number of datasets are available. These differ in their properties, such as geographic location of mining and production, TRL, V_2O_5 source, degree of product purity or LCA scope, resulting in a GWP ranging from 1 to 115 kg CO_2-eq/kg V_2O_5. This demonstrates that it is crucial to carefully examine the used V_2O_5 dataset for quality and applicability, as different datasets can lead to strongly differing overall LCIA results for VRFB production and the entire HESS lifecycle. Environmental impacts of vanadium electrolyte modeled with three selected V_2O_5 datasets from literature, two of which primary and one secondary, were compared. It was observed that V_2O_5, regardless of the selected dataset, caused the highest share of environmental impacts of electrolyte production in most midpoint categories.

Moreover, a recycling process for waste vanadium electrolyte was developed on laboratory scale, to investigate its potential for emission reduction of the HESS. In a semi-automated plant, a recycling efficiency of 81.6 % by amount of vanadium and a final product with a total vanadium concentration of 1.75 mol/l were achieved. The recycled electrolyte was suitable for direct use in a VRFB. The GWP of recycled electrolyte at a vanadium concentration of 1.6 mol/l was 0.91 kg CO_2-eq/kg, being lower than that of electrolyte prepared with V_2O_5 from most primary sources.

Eventually, the environmental impacts of the entire HESS lifecycle were analyzed in twelve scenarios, obtaining an overall GWP between 0.10 and 0.53 kg CO_2-eq/kWh. This assessment revealed that V_2O_5 and the electricity losses during charging and discharging represented the main environmental hotspots. The scenario analysis demonstrated that the overall impacts of the HESS could be significantly reduced, if recycled electrolyte was used for the VRFB instead of primary one and if charging was done with renewable electricity sources instead of a conventional grid mix.

In a sensitivity analysis, the effects of an alteration of the system's storage efficiency on its environmental impacts were investigated. The effects depended on the parameters of the HESS: They were higher when using primary V_2O_5 and conventional grid power for charging and less pronounced with recycled electrolyte and renewable electricity.

Future efforts regarding a roll-out of this new technology need to focus on the exploitation and LCA of secondary V_2O_5 sources and on the establishment of a circular economy for vanadium electrolyte, specifically in Europe. Additionally, the HESS should be limited to renewables applications. Combined with further research into enhancing the system's storage efficiency, this approach would allow for a reduction of the environmental impacts associated with the storage losses of the HESS.

CRediT authorship contribution statement

Eva-Maria Heigl: Writing – review & editing, Writing – original draft, Visualization, Methodology, Investigation, Formal analysis, Data curation, Conceptualization. **Michael Schäffer:** Writing – review & editing, Writing – original draft, Visualization, Methodology, Formal analysis, Data curation. **Lukas Zeilerbauer:** Writing – review & editing, Validation. **Andreas Zauner:** Investigation, Formal analysis. **Johannes Lindorfer:** Writing – review & editing, Validation. **Johannes Ott:** Writing – review & editing, Investigation, Formal analysis, Data curation. **Peter Fischer:** Writing – review & editing, Writing – original draft, Visualization, Methodology, Formal analysis, Data curation.

Declaration of Generative AI and AI-assisted technologies in the writing process

During the preparation of this work the author(s) used ChatGPT in order to enhance the readability respectively the wording of a few text passages. After using this tool, the author(s) reviewed and edited the content as needed and take(s) full responsibility for the content of the publication.

Declaration of competing interest

The authors declare that they have no known competing financial interests or personal relationships that could have appeared to influence the work reported in this paper.

Acknowledgments

This project has received funding from the European Union's Horizon 2020 research and innovation program under grant agreement No. 963550. The authors would like to thank all members of the HyFlow project consortium for providing extensive data that form the basis of this study and for valuable expert-input and discussions throughout the project and in the process of establishing this publication.

This publication includes content supplied by the LCA databases Sphera [45] and ecoinvent [46] or their third party providers.

Appendix A. Supplementary data

Supplementary data to this article can be found online at https://doi.org/10.1016/j.est.2025.117705.

Data availability

Underlying data are provided in the Supplementary Information.

References

[1] European Commission, The European Green Deal. [Online], Available: https://commission.europa.eu/strategy-and-policy/priorities-2019-2024/european-green-deal/energy-and-green-deal_en (accessed: Jul. 4 2024).
[2] S. Passerini, L. Barelli, M. Baumann, J. Peters, Marcel Weil (Eds.), Emerging Battery Technologies to Boost the Clean Energy Transition: Cost, Sustainability, and Performance Analysis, 1st ed., Springer International Publishing, Cham, 2024. Accessed: Jan. 23 2025. [Online]. Available: https://link.springer.com/book/10.1007/978-3-031-48359-2.
[3] Regulation (EU) 2023/1542 of the European Parliament and of the Council of 12 July 2023 concerning batteries and waste batteries, amending Directive 2008/98/EC and Regulation (EU) 2019/1020 and repealing Directive 2006/66/EC: Batteries Regulation, Accessed: Jul. 4 2024. [Online]. Available: https://eur-lex.europa.eu/eli/reg/2023/1542/oj, 2023.
[4] United Nations, 17 Sustainable Development Goals (SDG): 2030 Agenda for Sustainable Development. [Online], Available: https://sdgs.un.org/goals (accessed: Jul. 16 2024).
[5] United Nations, The Paris Agreement: International Treaty on Climate Change. [Online], Available: https://unfccc.int/process-and-meetings/the-paris-agreement (accessed: Jul. 16 2024).
[6] European Commission, Waste and Recycling: Batteries. [Online], Available: https://environment.ec.europa.eu/topics/waste-and-recycling/batteries_en (accessed: Jul. 4 2024).
[7] Haoyang He, Shan Tian, Brian Tarroja, Oladele A. Ogunseitan, Scott Samuelsen, Julie M. Schoenung, Flow battery production: materials selection and environmental impact, J. Clean. Prod. 269 (Oct. 2020) 121740, https://doi.org/10.1016/j.jclepro.2020.121740.
[8] Michael Dieterle, Peter Fischer, Marie-Noelle Pons, Nick Blume, Christine Minke, Aldo Bischi, Life cycle assessment (LCA) for flow batteries: a review of methodological decisions, Sustain. Energy Technol. Assess. 30 (Part A) (Oct. 2022), https://doi.org/10.1016/j.seta.2022.102457, 2213-1388.
[9] Christina Roth, Jens Noack, Maria Skyllas-Kazacos (Eds.), Flow Batteries. From Fundamentals to Applications, 2023rd ed., Wiley-VCH, Weinheim, Germany, 2023. Accessed: Jan. 23 2025. [Online]. Available: https://doi.org/10.1002/9783527832767.
[10] Abdul Ghani Olabi, Qaisar Abbas, Pragati A. Shinde, Mohammad Ali Abdelkareem, Rechargeable batteries: technological advancement, challenges, current and emerging applications, Energy 266 (Mar. 2023) 126408, https://doi.org/10.1016/j.energy.2022.126408.
[11] Sophie Ebner, Stefan Spirk, Tobias Stern, Claudia Mair-Bauernfeind, How green are redox flow batteries? ChemSusChem 16 (8) (2023) [Online]. Available: https://doi.org/10.1002/cssc.202201818.
[12] G. Smdani, M.R. Islam, A.N. Ahmad Yahaya, S.I. Bin Safie, Performance evaluation of advanced energy storage systems: a review, Energy & Environment 34 (4) (2023) 1094–1141 [Online]. Available: https://doi.org/10.1177/0958305X2210747.
[13] Mohammad Amir, Radhika G. Deshmukh, Haris M. Khalid, Zafar Said, S.M. Ali Raza, Abdul-Sattar Nizami Muyeen, Rajvikram Madurai Elavarasan, R. Saidur, Kamaruzzaman Sopian, Energy storage technologies: an integrated survey of developments, global economical/environmental effects, optimal scheduling model, and sustainable adaption policies, J Energy Storage 72 (Part E) (2023) 108694, https://doi.org/10.1016/j.est.2023.108694.
[14] Hafsah A. Khan, Muhammad Tawalbeh, Bashar Aljawrneh, Waad Abuwatfa, Amani Al-Othman, Hasan Sadeghifa, Abdul Ghani Olabi, A comprehensive review on supercapacitors: their promise to flexibility, high temperature, materials, design, and challenges, Energy 295 (2024) 131043, https://doi.org/10.1016/j.energy.2024.131043.
[15] Mustafa Ergin Sahin, Frede Blaabjerg, Ariya Sangwongwanich, A comprehensive review on supercapacitor applications and developments, Energies 15 (3) (2022) 674 [Online]. Available: https://doi.org/10.3390/en15030674.
[16] Eduardo Sánchez-Díez, Edgar Ventosa, Massimo Guarnieri, Andrea Trovò, Cristina Flox, Rebeca Marcilla, Francesca Soavi, Petr Mazur, Estibaliz Aranzabe, Raquel Ferret, Redox flow batteries: status and perspective towards sustainable stationary energy storage, J. Power Sources 481 (2021) 228804, https://doi.org/10.1016/j.jpowsour.2020.228804.
[17] Mustafa Ergin Şahin, Frede Blaabjerg, A review on supercapacitor materials and developments, Turkish Journal of Materials 5 (2) (2020) 10–24 [Online]. Available: https://vbn.aau.dk/ws/portalfiles/portal/407249324/166_838_1_PB.pdf.
[18] Horizon, HyFlow: development of a sustainable hybrid storage system based on high power vanadium redox flow battery and supercapacitor – technology: Grant agreement ID: 963550 [Online]. Available: https://cordis.europa.eu/project/id/963550, 2020 https://hyflow-h2020.eu/.
[19] Lígia da Silva Lima, Mattijs Quartier, Astrid Buchmayr, David Sanjuan-Delmás, Hannes Laget, Dominique Corbisier, Jan Mertens, Jo Dewulf, Life cycle assessment of lithium-ion batteries and vanadium redox flow batteries-based renewable energy storage systems, Sustain. Energy Technol. Assess. 46 (2021) 101286, 2213-1388. [Online]. Available: https://www.sciencedirect.com/science/article/pii/S2213138821002964.
[20] Nick Blume, Maik Becker, Thomas Turek, Christine Minke, Life cycle assessment of an industrial-scale vanadium flow battery, J. Ind. Ecol. 26 (2022) 1796–1808, https://doi.org/10.1111/jiec.13328.
[21] Selina Weber, Jens F. Peters, Manuel Baumann, Marcel Weil, Life cycle assessment of a vanadium redox flow battery, Environ. Sci. Technol. 52 (18) (2018) 10864–10873 [Online]. Available: https://pubs.acs.org/doi/10.1021/acs.est.8b02073.
[22] J. Gouveia, A. Mendes, R. Monteiro, T.M. Mata, N.S. Caetano, A.A. Martins, Life cycle assessment of a vanadium flow battery: The 6th International Conference on Energy and Environment Research - Energy and environment: challenges towards circular economy, July 22–25, 2019, University of Aveiro, Portugal, Energy Rep. 6 (Suppl. 1) (2020) 95–101 [Online]. Available: https://doi.org/10.1016/j.egyr.2019.08.025.
[23] Yanxin Li, Xiaoqu Han, Lu Nie, Yelin Deng, Junjie Yan, Tryfon C. Roumpedakis, Dimitrios-Sotirios Kourkoumpas, Sotirios Karellas, Life cycle environmental hotspots analysis of typical electrochemical, mechanical and electrical energy storage technologies for different application scenarios: Case study in China, J. Clean. Prod. 446 (2024) 142862, https://doi.org/10.1016/j.jclepro.2024.142862.
[24] Xiaoqu Han, Lu Yanxin Li, Xiaofan Huang Nie, Yelin Deng, Junjie Yan, Dimitrios-Sotirios Kourkoumpas, Sotirios Karellas, Comparative life cycle greenhouse gas emissions assessment of battery energy storage technologies for grid applications, J. Clean. Prod. 392 (2023) 136251, https://doi.org/10.1016/j.jclepro.2023.136251.
[25] Matteo Cossutta, Viliam Vretenar, Teresa A. Centeno, Peter Kotrusz, Jon McKechnie, Stephen J. Pickering, A comparative life cycle assessment of graphene and activated carbon in a supercapacitor application, J. Clean. Prod. 242 / 118468 (Jan. 2020) [Online]. Available: https://doi.org/10.1016/j.jclepro.2019.118468.
[26] D.M. Yang Jiao, Greenhouse gas emissions from hybrid energy storage systems in future 100% renewable power systems – a Swedish case based on consequential life cycle assessment, J Energy Storage 57 / 106167 (2023) [Online]. Available: https://doi.org/10.1016/j.est.2022.106167.
[27] A. Kamal Kamali, Edis Glogic, Nilanka M. Keppetipola, Guido Sonnemann, Thierry Toupance, Ludmila Cojocaru, Prospective life cycle assessment of two supercapacitor architectures, Sustainable Chemistry & Engineering 11 (2023) 15898–15909 [Online]. Available: https://doi.org/10.1021/acssuschemeng.3c04007?urlappend=%3Fref%3DPDF&jav=VoR&rel=cite-as.
[28] European Commission, Critical raw materials [Online]. Available: https://single-market-economy.ec.europa.eu/sectors/raw-materials/areas-specific-interest/critical-raw-materials_en (accessed: Jul. 4 2024).
[29] Proposal for a REGULATION OF THE EUROPEAN PARLIAMENT AND OF THE COUNCIL establishing a framework for ensuring a secure and sustainable supply of critical raw materials and amending Regulations (EU) 168/2013, (EU) 2018/858, 2018/1724 and (EU) 2019/1020: COM/2023/160 final [Online]. Available: https://eur-lex.europa.eu/legal-content/EN/TXT/?uri=CELEX%3A52023PC0160, 2023.
[30] COMMUNICATION FROM THE COMMISSION TO THE EUROPEAN PARLIAMENT, THE COUNCIL, THE EUROPEAN ECONOMIC AND SOCIAL COMMITTEE AND THE COMMITTEE OF THE REGIONS on the 2017 list of Critical Raw Materials for the EU: COM/2017/0490 Final, Accessed: Jul. 4 2024. [Online]. Available: https://eur-lex.europa.eu/legal-content/EN/TXT/?uri=CELEX:52017DC0490, 2017.
[31] Amirreza Nasimifar, Javad Vazife Mehrabani, A review on the extraction of vanadium pentoxide from primary, secondary, and co-product sources, International Journal of Minining and Geo-Engineering 56-4 (2022) 361–382 [Online]. Available: https://doi.org/10.22059/ijmge.2022.319012.594893.
[32] Guangming Zhang, Yuting Wang, Xianhao Meng, Di Zhang, Ning Ding, Zhijun Ren, Wenfang Gao, Zhi Sun, Life cycle assessment on the vanadium production process: a multi-objective assessment under environmental and economic perspectives, Resour. Conserv. Recycl. 192 / 10626 (May. 2023) [Online]. Available: https://doi.org/10.1016/j.resconrec.2023.106926.
[33] M. Petranikova, A.H. Tkaczyk, A. Bartl, A. Amato, V. Lapkovskis, C. Tunsu, Vanadium sustainability in the context of innovative recycling and sourcing

development, Waste Manag. 113 (2020) 521–544 [Online]. Available: https://doi.org/10.1016/j.wasman.2020.04.007.
[34] Pritil Gunjan, Maria Chavez, Dan Power, White Paper: Vanadium Redox Flow Batteries: Identifying Market Opportunities and Enablers: By Order of the Company "Vanitec", Guidehouse Inc., Guidehouse Insights, 2022. Q2. [Online]. Available: https://vanitec.org/images/uploads/Guidehouse_Insights-Vanadium_Redox_Flow_Batteries.pdf.
[35] The International Energy Agency (IEA), World Energy Outlook 2023, France. Accessed: Jan. 23 2025. [Online]. Available: https://www.iea.org/reports/world-energy-outlook-2023?wpappninja_v=b64a7tp1d, 2023.
[36] K.E. Rodby, T.J. Carney, Y. Ashraf Gandomi, J.L. Barton, R.M. Darling, F. R. Brushett, Assessing the levelized cost of vanadium redox flow batteries with capacity fade and rebalancing, J. Power Sources 460 (2020) 227958, https://doi.org/10.1016/j.jpowsour.2020.227958.
[37] Nick Blume, Oliver Zielinski, Maik Becker, Christine Minke, Prospective life cycle assessment of chemical electrolyte recycling for vanadium flow batteries: a comprehensive study, Energy Technology 12 (2024), https://doi.org/10.1002/ente.202300750.
[38] ISO 14040:2006(en), Environmental management - Life Cycle Assessment - Principles and Framework, International Organization for Standardization, 2006 [Online]. Available: https://www.iso.org/obp/ui/.
[39] ISO 14044:2006(en), Environmental Management - Life Cycle Assessment - Requirements and Guidelines, International Organization for Standardization, 2006 [Online]. Available: https://www.iso.org/obp/ui/.
[40] Rolf Frischknecht, Lehrbuch der Ökobilanzierung, Springer Spektrum, Berlin, 2020 [Online]. Available: https://link.springer.com/book/10.1007/978-3-662-54763-2.
[41] J.B. Guinée, M. Gorrée, R. Heijungs, G. Huppes, R. Kleijn, A. de Koning, L. van Oers, A. Wegener Sleeswijk, S. Suh, H.A. Udo de Haes, H. de Bruijn, R. van Duin, M. Huijbregts, Handbook on Life Cycle Assessment. Operational Guide to the ISO Standards, 1st ed, Springer Dordrecht, Dordrecht, 2002 [Online]. Available: https://doi.org/10.1007/0-306-48055-7.
[42] Mary Ann Curran (Ed.), Life Cycle Assessment Handbook. A Guide for Environmentally Sustainable Products, Wiley, 2012 [Online]. Available: https://onlinelibrary.wiley.com/doi/book/10.1002/9781118528372.
[43] B.G. Walter Klöpffer, Life Cycle Assessment (LCA). A Guide to Best Practice, Wiley-VCH, Weinheim, Germany, 2014. Accessed: Jan. 22 2025. [Online]. Available: https://doi.org/10.1002/9783527655625.
[44] Flaticon [Online]. Available: flaticon.com.
[45] Sphera, GaBi ts 10.7 Software and Professional Database [Online]. Available: https://sphera.com/software-fuer-die-lebenszyklus-beurteilung-lca/?lang=de (accessed: Feb. 20 2023).
[46] ecoinvent Association, Ecoinvent Database: Sustainability Assessment [Online]. Available: https://ecoinvent.org/database/ (accessed: Feb. 20 2024).
[47] Shuangyin Chen, Fu Xiaojiao, Mansheng Chu, Zhenggen Liu, Jue Tang, Life cycle assessment of the comprehensive utilisation of vanadium titano-magnetite, J. Clean. Prod. 101 (2015) 122–128 [Online]. Available: https://doi.org/10.1016/j.jclepro.2015.03.076.
[48] N. Jungbluth, S. Eggenberger, Life Cycle Assessment for Vanadium Pentoxide (V2O5) From Secondary Resources, ESU-services Ltd, 2018.
[49] He Li, Hailin Tian, Ting-Hsiang Chang, Jianyi Zhang, Shin Nuo Koh, Xiaonan Wang, Chi-Hwa Wang, Po-Yen Chen, High-purity V2O5 Nanosheets synthesized from gasification waste: flexible energy storage devices and environmental assessment, ACS Sustain. Chem. Eng. 7 (2019) 12474–12484 [Online]. Available: https://doi.org/10.1021/acssuschemeng.9b02066.
[50] Sina Shakibania, Alireza Mahmoudi, Fereshteh Rashchi, Ehsan Vahidi, Recovery of vanadium from spent refinery catalysts: optimizing the process and analyzing the environmental impact, Clean Techn. Environ. Policy 26 (Nov. 2023), 291–30. [Online]. Available: https://doi.org/10.1007/s10098-023-02628-7.
[51] M. Baritto, A.O. Oni, A. Kumar, Life cycle GHG emissions assessment of vanadium recovery from bitumen-derived petcoke fly ash, J. Environ. Manag. 363 (2024) 121377 [Online]. Available: https://doi.org/10.1016/j.jenvman.2024.121377.
[52] A. Edis Glogic, Kamal Kamali, Nilanka M. Keppetipola, G.R. Babatunde Alonge, Asoka Kumara, Guido Sonnemann, Thierry Toupance, Ludmila Cojocaru, Life cycle assessment of supercapacitor electrodes based on activated carbon from coconut shells, ACS Sustain. Chem. Eng. 10 (46) (2022) 15025–15034 [Online]. Available: https://doi.org/10.1021/acssuschemeng.2c03239.
[53] Y. Wang, J. Wang, X. Zhang, D. Bhattacharyya, E.M. Sabolsky, Quantifying environmental and economic impacts of highly porous activated carbon from lignocellulosic biomass for high-performance supercapacitors, Energies (2022) 15–351 [Online]. Available: https://doi.org/10.3390/en15010351.
[54] Xiefei Zhu, Claudia Labianca, Mingjing He, Zejun Luo, Wu Chunfei, Siming You, Daniel C.W. Tsang, Life-cycle assessment of pyrolysis processes for sustainable production of biochar from agro-residues, Bioresour. Technol. 360 (2022) 127601 [Online]. Available: https://doi.org/10.1016/j.biortech.2022.127601.
[55] Shashank Sundriyal, Vishal Shrivastav, Hong Duc Pham, Sunita Mishra, Akash Deep, Deepak P. Dubal, Advances in bio-waste derived activated carbon for supercapacitors: Trends, challenges and prospective, Resour. Conserv. Recycl. 169 (2021) 105548 [Online]. Available: https://doi.org/10.1016/j.resconrec.2021.105548.
[56] Atakan Kocanali Kuray Dericiler, Merve Buldu-Akturk, Emre Erdem, Burcu Saner Okan, Upcycling process of transforming waste coffee into spherical graphene by flash pyrolysis for sustainable supercapacitor manufacturing with virgin graphene electrodes and its comparative life cycle assessment, Biomass Convers. Biorefinery 14 (2024) 1073–1088 [Online]. Available: https://doi.org/10.1007/s13399-022-02447-8.
[57] Matteo Cossutta, Life Cycle Analysis of Graphene in a Supercapacitor Application, PhD thesis, University of Nottingham, 2015. Accessed: Jul. 5 2024. [Online]. Available: https://eprints.nottingham.ac.uk/33411/.
[58] Elisabetta Petri, Eva-Maria Heigl, Andrea Fasolini, Lukas Zeilerbauer, Monica Giovannucci, Yusuf Küçükağa, Cristian Torri, Francesco Basile, Francesca Soavi, Conversion of biodigestate into activated carbon for electrochemical application: process performance and life cycle assessment, Carbon 226 (2024) 119221 [Online]. Available: https://doi.org/10.1016/j.carbon.2024.119221.
[59] T.S. Bhat, P.S. Patil, R.B. Rakhi, Recent trends in electrolytes for supercapacitors, Journal of Energy Chemistry 50 (2022) 104222 [Online]. Available: https://doi.org/10.1016/j.est.2022.104222.
[60] Institut für Arbeitsschutz der Deutschen Gesetzlichen Unfallversicherung, GESTIS-Stoffdatenbank: Acetonitrile [Online]. Available: https://gestis.dguv.de/data?name=013660&lang=en (accessed: Jul. 4 2024).
[61] E.O. Karan Bhuwalka, Memo on Nickel Market Dynamics and the Security of the Battery Supply Chain, Accessed: Jul. 16 2024. [Online]. Available: https://sites.utexas.edu/mineralstransition/files/2024/06/Nickel_Memo_Bhuwalka_Olivetti-Google-Docs.pdf, 2024.
[62] Ayman Elshkaki, Barbara K. Reckm, T.E. Graedel, Anthropogenic nickel supply, demand and associated energy and water use, Resour. Conserv. Recycl. 125 (Oct. 2017) 300–307 [Online]. Available: https://www.sciencedirect.com/science/article/pii/S0921344917301817.
[63] European Commission, "COMMUNICATION FROM THE COMMISSION TO THE EUROPEAN PARLIAMENT, THE COUNCIL, THE EUROPEAN ECONOMIC AND SOCIAL COMMITTEE AND THE COMMITTEE OF THE REGIONS Critical Raw Materials Resilience: Charting a Path Towards Greater Security and Sustainability: COM/2020/474 Final," Sep. 2020. Accessed: Jul. 4 2024. [Online]. Available: https://eur-lex.europa.eu/legal-content/EN/TXT/?uri=CELEX:52020DC0474.
[64] European Commission, Study on the Critical Raw Materials for the EU 2023: Final Report, Accessed: Jul. 4 2024. [Online]. Available: https://op.europa.eu/en/publication-detail/-/publication/57318397-fdd4-11ed-a05c-01aa75ed71a1.
[65] Mark Mistry, Johannes Gediga, Shannon Boonzaier, Life cycle assessment of nickel products, Int. J. Life Cycle Assess. 21 (2016) 1559–1572 [Online]. Available: https://link.springer.com/article/10.1007/s11367-016-1085-x.
[66] Matthew J. Eckelman, Facility-level energy and greenhouse gas life-cycle assessment of the global nickel industry, Resour. Conserv. Recycl. 54 (2010) 256–266 [Online]. Available: https://www.sciencedirect.com/science/article/pii/S0921344909001852.
[67] Barbara K. Reck, Daniel B. Müller, Katherine Rostkowski, T.E. Graedel, Anthropogenic nickel cycle: insights into use, trade and recycling, Environ. Sci. Technol. 42 (2008) 3394–3400 [Online]. Available: https://pubs.acs.org/doi/epdf/10.1021/es072108l.
[68] Eva Quéheille, Anne Ventura, Nadja Saiyouri, Franck Taillandier, A Life Cycle Assessment model of end-of-life scenarios for building deconstruction and waste management, J. Clean. Prod. 339 (2022) 130694 [Online]. Available: https://doi.org/10.1016/j.jclepro.2022.130694.
[69] Stefan Windisch-Kern, Eva Gerold, Thomas Nigl, Aleksander Jandric, Michael Altendorfer, Bettina Rutrecht, Silvia Scherhaufer, Harald Raupenstrauch, Roland Pomberger, Helmut Antrekowitsch, Florian Part, Recycling chains for lithium-ion batteries: a critical examination of current challenges, opportunities and process dependencies, Waste Manag. 138 (2022) 125–139 [Online]. Available: https://doi.org/10.1016/j.wasman.2021.11.038.
[70] Stephen Andreas Grot, Robert Moore, Recycling of NAFION(™) Ion Exchange Membranes: Opportunities and Challenge (invited) [Online]. Available: https://iopscience.iop.org/article/10.1149/MA2021-02601796mtgabs (accessed: Dec. 18 2023).
[71] Yutong Han, The Recycling of Commercial Nafion Membranes and Synthesis of High Performance Nafion Composite Membranes, Politecnico Milano, 2020. /21. Accessed: Dec. 18 2023. [Online]. Available: https://hdl.handle.net/10589/184939.
[72] Andrew Park, Sustainable Nafion(TM): Opportunities in Recycling & Re-use of Membranes and Ionomers: Manufacturing Automation and Recycling for Clean Hydrogen Technologies Experts Meeting [Online]. Available: https://www.energy.gov/sites/default/files/2022-07/h2-mach-16-park.pdf (accessed: Dec. 18 2023).
[73] M.A.J. Huijbregts, Z.J.N. Steinmann, P.M.F. Elshout, G. Stam, F. Verones, M.D. M. Vieira, A. Hollander, M. Zijp, R. van Zelm, ReCiPe 2016 v1.1: A Harmonized Life Cycle Impact Assessment Method at Midpoint and Endpoint Level: Report I: Characterization, Ministry of Health, Welfare and Sport, The Netherlands, 2017 [Online]. Available: https://rivm.openrepository.com/handle/10029/620793.
[74] Mark A.J. Huijbregts, Zoran J.N. Steinmann, Pieter M.F. Elshout, Gea Stam, ReCiPe2016: a harmonised life cycle impact assessment method at midpoint and endpoint level, Int. J. Life Cycle Assess. 22 (2017) 138–147, https://doi.org/10.1007/s11367-016-1246-y.
[75] Thilo Kupfer, et al., GaBi Databases & Modelling Principles [Online]. Available: www.sphera.com, 2021.
[76] VDI 4600 Kumulierter Energieaufwand - Begriffe, Definitionen, Berechnungsmethoden, VDI, 1997.
[77] L.I. Xing-bin, W.E.I. Chang, W.U. Jun, L.I. Cun-xiong, L.I. Min-ting, D.E.N.G. Zhi-gan, X.U. Hong-sheng, Thermodynamics and mechanism of vanadium(IV) extraction from sulphate medium with D2EHPA, EHEHPA and CYANEX 272 in kerosene, Trans. Nonferrous Metals Soc. China 22 (2012) 461–466 [Online]. Available: https://doi.org/10.1016/S1003-6326(11)61199-0.
[78] Qihua Shi, Yimin Zhang, Jing Huang, Tao Liu, Hong Liu, Luyao Wang, Synergistic solvent extraction of vanadium from leaching solution of stone coal using D2EHPA

and PC88A, Sep. Purif. Technol. 118 (2017) 1–7 [Online]. Available: https://doi.org/10.1016/j.seppur.2017.03.010.
[79] C.A. Blake, K.B. Brown, C.F. Coleman, The Extraction and Recovery of Uranium (and Vanadium) from Acid Liquors with di(2-Ethylhexyl) Phosphoric Acid and some Other Organophosphorus Acids, Metallurgy-Raw Materials ORNL-1903, Oak Ridge National Laboratory, USA, 1955. Accessed: Aug. 21 2024. [Online]. Available: https://www.osti.gov/servlets/purl/4385766.
[80] Danick Reynard, Heron Vrubel, Christopher R. Dennison, Alberto Battistel, Hubert Girault, On-site purification of copper-contaminated vanadium electrolytes by using a vanadium redox flow battery, ChemSusChem 12 (2019) 1222–1228, https://doi.org/10.1002/cssc.201802895.
[81] M. Pahlevaninezhad, M. Pahlevani, E.P. Roberts, Effects of aluminum, iron, and manganese sulfate impurities on the vanadium redox flow battery, J. Power Sources 529 (2022) 231271, https://doi.org/10.1016/j.jpowsour.2022.231271.
[82] Fabiano Piccinno, Roland Hischier, Stefan Seeger, Claudia Som, From laboratory to industrial scale: a scale-up framework for chemical processes in life cycle assessment studies, J. Clean. Prod. 135 (2016) 1085–1097 [Online]. Available: https://doi.org/10.1016/j.jclepro.2016.06.164.
[83] Cellcube, Whitepaper: Environmental Impact, VRFB vs. LiB, Enerox GmbH, Dec. 2022 [Online]. Available: www.cellcube.com.
[84] Nick Blume, Magdalena Neidhart, Pavel Mardilovich, Christine Minke, Life cycle assessment of a vanadium flow battery based on manufacturer data: 30th CIRP Life Cycle Engineering Conference, Procedia CIRP 116 (2023) 648–653 [Online]. Available: https://doi.org/10.1016/j.procir.2023.02.109.
[85] Maxwell Technologies Inc, Datasheet of 2.7V 5F ULTRACAPACITOR CELL [Online]. Available: https://maxwell.com/wp-content/uploads/2021/08/2_7_5F_ds_3001974_datasheet.pdf (accessed: Feb. 21 2024).
[86] Thomas Le Varlet, Oliver Schmidt, Ajay Gambhir, Sheridan Few, Iain Staffell, Comparative life cycle assessment of lithium-ion battery chemistries for residential storage, J Energy Storage 28 (2020) 101230 [Online]. Available: https://doi.org/10.1016/j.est.2020.101230.
[87] C.F. Blanco, P. Behrens, M. Vijver, W. Peijnenburg, J. Quik, S. Cucurachi, A framework for guiding safe and sustainable-by-design innovation, J. Ind. Ecol. 29 (1) (2025) 47–65, https://doi.org/10.1111/jiec.13609.
[88] J. Šimaitis, I. Butnar, R. Sacchi, R. Lupton, C. Vagg, S. Allen, Expanding scenario diversity in prospective LCA: Coupling the TIAM-UCL integrated assessment model with premise and ecoinvent, Renew. Sust. Energ. Rev. 211 (2025) 115298, https://doi.org/10.1016/j.rser.2024.115298.
[89] V. Bisinella, T.H. Christensen, T.F. Astrup, Future scenarios and life cycle assessment: systematic review and recommendations, Int. J. Life Cycle Assess. 26 (11) (2021) 2143–2170, https://doi.org/10.1007/s11367-021-01954-6.
[90] B.P. Weidema, M.S. Wesnæs, Data quality management for life cycle inventories—an example of using data quality indicators, J. Clean. Prod. 4 (3–4) (1996) 167–174, https://doi.org/10.1016/S0959-6526(96)00043-1.
[91] S. Muller, P. Lesage, R. Samson, Giving a scientific basis for uncertainty factors used in global life cycle inventory databases: An algorithm to update factors using new information, Int. J. Life Cycle Assess. 21 (8) (2016) 1185–1196, https://doi.org/10.1007/s11367-016-1098-5.
[92] S. Muller, P. Lesage, A. Ciroth, C. Mutel, B.P. Weidema, R. Samson, The application of the pedigree approach to the distributions foreseen in ecoinvent v3, Int. J. Life Cycle Assess. 21 (9) (2016) 1327–1337, https://doi.org/10.1007/s11367-014-0759-5.
[93] Bauer Weidema, Mutel Hischier, Reinhard Nemecek, Wernet Vadenbo, Overview and Methodology: Data Quality Guideline for the Ecoinvent Database Version 3: Ecoinvent Report 1 (v3), St. Gallen, 2013. Accessed: Jun. 18 2025. [Online]. Available: https://vbn.aau.dk/ws/portalfiles/portal/176769045/Overview_and_methodology.pdf.
[94] Jiyun Heo, Jae-Yun Han, Soohyun Kim, Seongmin Yuk, Chanyong Choi, Riyul Kim, Ju-Hyuk Lee, Andy Klassen, Shin-Kun Ryi, Hee-Tak Kim, Catalytic production of impurity-free V3.5+ electrolyte for vanadium redox flow batteries, Nat. Commun. 10 (2019) 4412 [Online]. Available: https://doi.org/10.1038/s41467-019-12363-7.
[95] S. Cucurachi, B. Steubing, F. Siebler, N. Navarre, C. Caldeira, S.P. Sala, Prospective LCA Methodology for Novel and Emerging Technologies for BIO-Based Products - the Planet Bio Project, Luxembourg JRC129632. Accessed: Aug. 21 2024. [Online]. Available: https://doi.org/10.2760/167543, 2022.
[96] The United Nations, Global Harmonized System (GHS) of Classification, Labelling and Packaging of Chemicals [Online]. Available: https://unece.org/about-ghs (accessed: Mar. 26 2025).